POLITECNICO DI TORINO

MASTER OF SCIENCE IN PETROLEUM AND MINING ENGINEERING

MASTER's DEGREE THESIS

Politecnico di Torino

Title

Geomechanical characteristics and karst of gypsum formations at Moncalvo quarry

Candidate

Muhammad Umer
S272626

Academic Supervisor(s)

Prof. Oggeri Claudio

Academic Co-Supervisor(s)
Prof. Adriano Fiorucci

Academic Year: 2023/2024

Abstract

A comprehensive literature review and experiment of the geomechanical characterization of gypsum in Moncalvo quarry is provided in this document. The topics covered are description of Moncalvo site, activities performed with in the quarry and the uses of gypsum. The documents provide an introduction of the Geological Strength Index (GSI), GSI functions, GSI values projected in ground and the GSI Classification system's precision. The measurement of all the properties of all fine grained and coarse grained specimens are highlighted in this work.

The geological layout of Moncalvo and Murisengo quarry is also discussed. In Piedmont Messinian age, the primary gypsum deposits are situated in the Monferrato region. Over the past centuries, a majority of these deposits have been mined, with only four quarries currently operational. The exposed gypsum-bearing formations exhibit distinct geological, structural, and hydrogeological characteristics that can impact the process of quarrying. We have obtained interesting results of the specimen's strength before and after testing in the Laboratory.

According to the observations and data collected from the Moncalvo quarry, the final consideration is related to the linear elastic part as this part is evidence. It is possible to set stress and strain and this we assume is equal to Modulus of Elasticity. We have calculated it both graphically and numerically because we have all the data coming from graph.

Gypsum, an evaporitic mineral, holds significant importance in various fields such as structural geology and civil engineering. It plays a crucial role in orogenetic tectonics and influences basin dynamics. Moreover, it is closely associated with economic activities including oil exploration, mining, and waste repositories. For instance, studies by Heard and Rubey (1966), de Meer and Spiers (1999), Cristallini and Ramos (2000), Zucali et al. (2010), and Liang et al. (2012) have highlighted its multifaceted roles.

Underground mining operations involving gypsum frequently encounter challenges such as roof collapses, pillar failures, water inrushes, and surface subsidence. These issues are particularly pronounced in abandoned or older underground sites, exacerbated by unexpected water circulation. Noteworthy research by Bonetto et al. (2008), Wang et al. (2008), and Sadeghiamirshahidi and Vitton (2019) has delved into the complexities of these phenomena.

To mitigate environmental harm and ensure responsible utilization of gypsum resources, it's crucial to prioritize water resource conservation and assess hazards linked to karst activity. Additionally, comprehensive measures for local geostructural surveying, geomechanical characterization, and ongoing stope monitoring, particularly focusing on deformation, should be systematically incorporated to ensure the safety of design plans.

Acknowledgements

This thesis concludes my master's degree. During this journey I have come across some excellent professors. I would like to express my deepest gratitude to my supervisors, **Professor Oggeri Claudio and Professor Adriano Fiorucci** who guided me throughout this thesis work and without them it would not have been possible. I am thankful to my supervisors for their continued support.

I would also like to thank all my friends and family who supported me spiritually in this time of need. I would like to thank them for believing in me. In the end, I would like to pay my regards to my colleagues of Politecnico Di Torino for the affection they showed throughout.

SUMMARY

Contents

CHAPTER 01

1.1 DESCRIPTION OF SITE

1) INTRODUCTION

Karst is the term used to characterize the gradual dissolution of soluble rocks like carbonates, evaporates, and halite by water that has been enriched with carbon dioxide. Dolines and sinkholes are the most prevalent types of typical landforms, which reflect morphological effects at the surface. The soluble rocks below the surface dissolve into conduits of various sizes, creating a network of voids, of which the portions big enough for human exploration are referred to as caves. The word "karst" comes from the German translation of the regional appellation for the area between Slovenia and Italy (Carso in Italian, Kras in Slovene). At the close of the seventeenth century, this area served as the birthplace of the science of karstology. The word "karst" was first used in the international literature in 1893 thanks in large part to the research of academics like Cvijic. The carbonate rock outcrops that make up karst make up about 14% of the Earth's land area, according to recent estimates (Chen et al. 2017). Much of the karst in Europe is found beneath some of the most heavily populated areas of the continent like England, northern and southern France, parts of Germany, central Italy, eastern Spain, and the majority of the Mediterranean, where effective water resource management is particularly important. Karst terrains make up about 25% of the land surface on other regions, such as the Middle East and Central Asia. Primary economic advantages like drinking water and building materials are frequently found in these karst regions. Karst regions are important ecosystems with high biodiversity numbers (Brancelj & Culver 2005; Pipan & Culver 2013). Numerous caves and other natural phenomena have greatly boosted tourism, assisting in the economic growth of numerous nations (Ravbar & ebela 2015). Karst aquifers and other amazing natural resources can be found in karst landscapes, which is why they are so significant. Karst groundwater is essential today for the sustainable development of the economy in many nations and regions. Karst water resources have played a significant role in the historical and economic development of many regions (Parise & Sammarco 2015). Approximately 15% of the world's population presently receives their drinking water from karst aquifers, which are also the only water source in some areas [1].

2) Karst geology, geomorphology and

Speleogenesis

Karst landscapes are renowned for their exquisite beauty and high aesthetic value, which are frequently exhibited by stunning surface geomorphology and subterranean features that can be seen in caverns. Due to the fact that show caves are frequently among the most popular tourist destinations worldwide, karst landscapes are well known to a broad range of people. In recent years, many various academic fields have shown a great deal of interest in karst research. In contrast to the outside environment (the Earth's surface), where the same features are typically destroyed by a combination of natural (such as weathering,

erosion, or mass movements) and anthropogenic processes, caves have been recognized as places where remarkable remains and deposits are preserved. Numerous studies involving experts in biology, medicine, astrobiology, and planetary geology have begun in order to explore the bacteria and other species living in challenging environments and under unusual climatic and environmental conditions. The biodiversity of karst is increasingly being recognized as being of extreme importance (Boston & Northup 2017). Now, speleologists and karst and cave scientists work together to conduct numerous cave excursions and explorations in some of the most significant cave systems in the world. The morphology of underground channels can be scanned in great detail thanks to new technologies like LiDAR scanners. In recent decades, these study areas have produced a significant amount of data as well as numerous scientific papers, and there have been an increasing number of national and international congresses devoted to karst research and speleology. The cave environment has been identified as a possible setting for the development of space exploration mission simulations, and caves are excellent locations for astronaut training (Fig. 1).Over the past five years, a large number of astronauts from various space agencies around the world have trained in caves thanks to a special training program that the European Space Agency has created (Bessone et al. 2017) [2].

Figure 1 The European Space Agency's 2014 CAVES camp featured astronaut training at the Su Benti grotto in Sardinia, Italy. There are numerous operational and safety procedure comparisons between progression on ropes and extravehicular activities. (Recent advances in karst research: from theory to fieldwork and applications MARIO PARISE1,2, FRANCI GABROVSEK3, GEORG KAUFMANN4 &NATASA RAVBAR3 1Department of Earth and Environmental Sciences, University Aldo Moro, Bari, Italy 2National Research Council, IRPI, Bari, Italy 3Karst Research Institute ZRC SAZU, Titov trg 2, Postojna, Slovenia 4Institute of Geological Sciences, Geophysics Section, Freie Universität Berlin, Germany*Correspondence: mario.parise@uniba.it)[3]*

The study of karst landscapes and their characteristics is important for many other disciplines in addition to karst science. The number of scientists from numerous various disciplines who are interested in

conducting research in this extraordinary environment reflects the multidisciplinary nature of karst studies. Karst is important for oil research because carbonate rocks could contain large reservoirs with considerable economic value. We are learning more about the economic elements of karst through numerous studies. Karst-type reservoirs, which are composed of carbonate and evaporite formations with signs of pervasive dissolution and cave formation, infilling and collapse during subsequent burial, have been found in various parts of the globe (e.g. Wang et al. 2015; Uni Research 2016) [4].

3) Description of Site

Gypsum from the Formazione Gessoso Solfifera, also known as the Complesso Caotico della Valle Versa, is quarried underground by Fassa Bortolo S.p.A. in the Monferrato region north of Asti (Piedmont Region) (Fig. 2). For 35 km, this evaporite series grows out irregularly. The study area's general stratigraphy is comprised of marly clayey deposits of Tortonian age that are capped by a thin bed of evaporitic limestone that is less than 1 m thick, followed by a series of gypsum beds that are separated by marly layers that range in thickness from 0.3 to 3.0 m and are of Messinian age. These marl-gypsum sequences represent successive evaporite cycles with the deposition of fine material (marls) first, followed by the deposition of gypsum in an increasingly salty brine, typically exhibiting macrocrystals in the lower part and, as a result of increasing supersaturation, microcrystals at the end of the cycle (Vai and Ricchi Lucchi, 1977). Due to a significant Messinian post-evaporitic erosion surface that separates this succession from an underlying thick silty-argillaceous sequence of Upper Messinian-Pliocene age, the thickness of the entire evaporite sequence varies from a few meters to over 70 m [5].

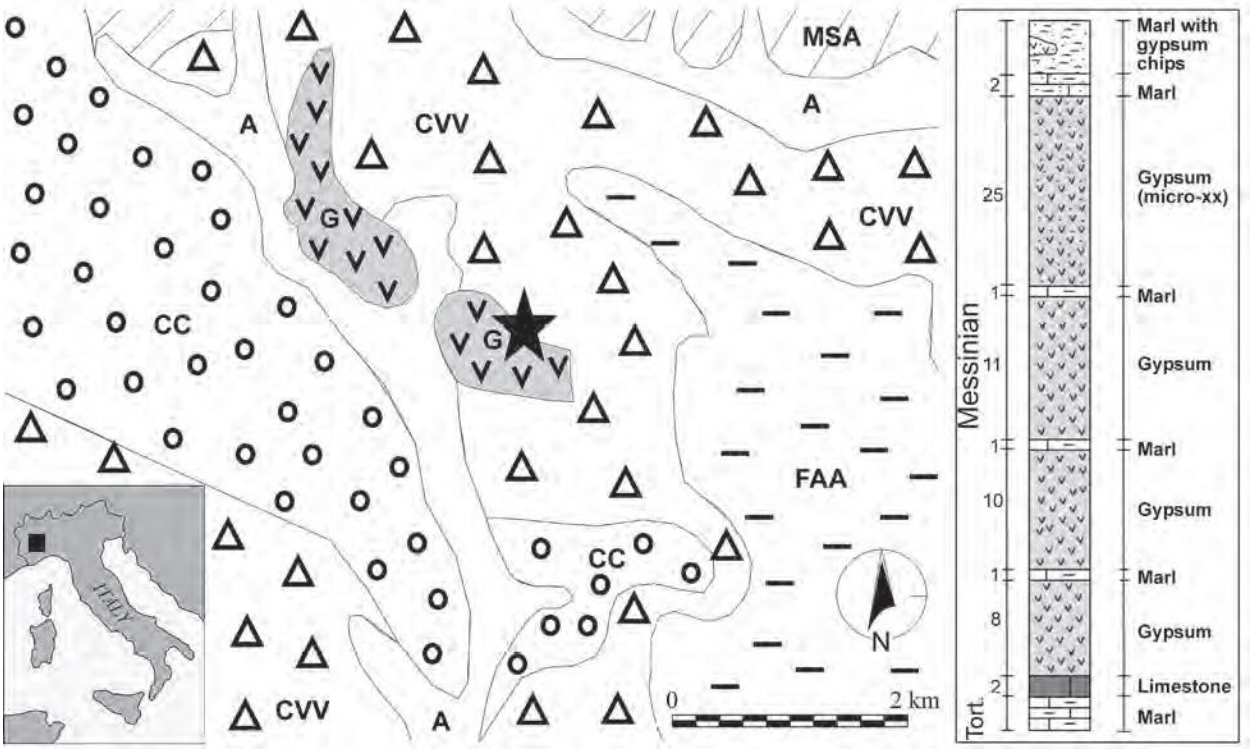

Figure 2 Simplified geological map and stratigraphic column of the study area (Conference paper January 2009, Messinian karst in Monferrato gypsum areas (North Italy) [6].

Stratigraphic column and a simplified geological map of the study region are shown in (Figure 2).

However, deep karst was thought to be only weakly developed in this poorly exposed gypsum formation until a large natural cavity was intercepted in an underground quarry near Moncalvo, resulting in a catastrophic collapse at the surface on February 15, 2005 (Fig. 3B) (Vigna et al., 2009). Small caves have been exposed in quarries in the upper gypsum layers, close to the surface (Fig. 3A). These 10 m-diameter voids, which are more than 1 km long and formed primarily below the level of the current thalwegs, are found in active phreatic conduits here. In several boreholes in other neighboring areas where gypsum is quarried underground, similar sizable phreatic voids have been discovered. In many quarries in the region, a thorough geomorphological and hydrogeological study has been conducted to try and comprehend the origin and development of these voids [7].

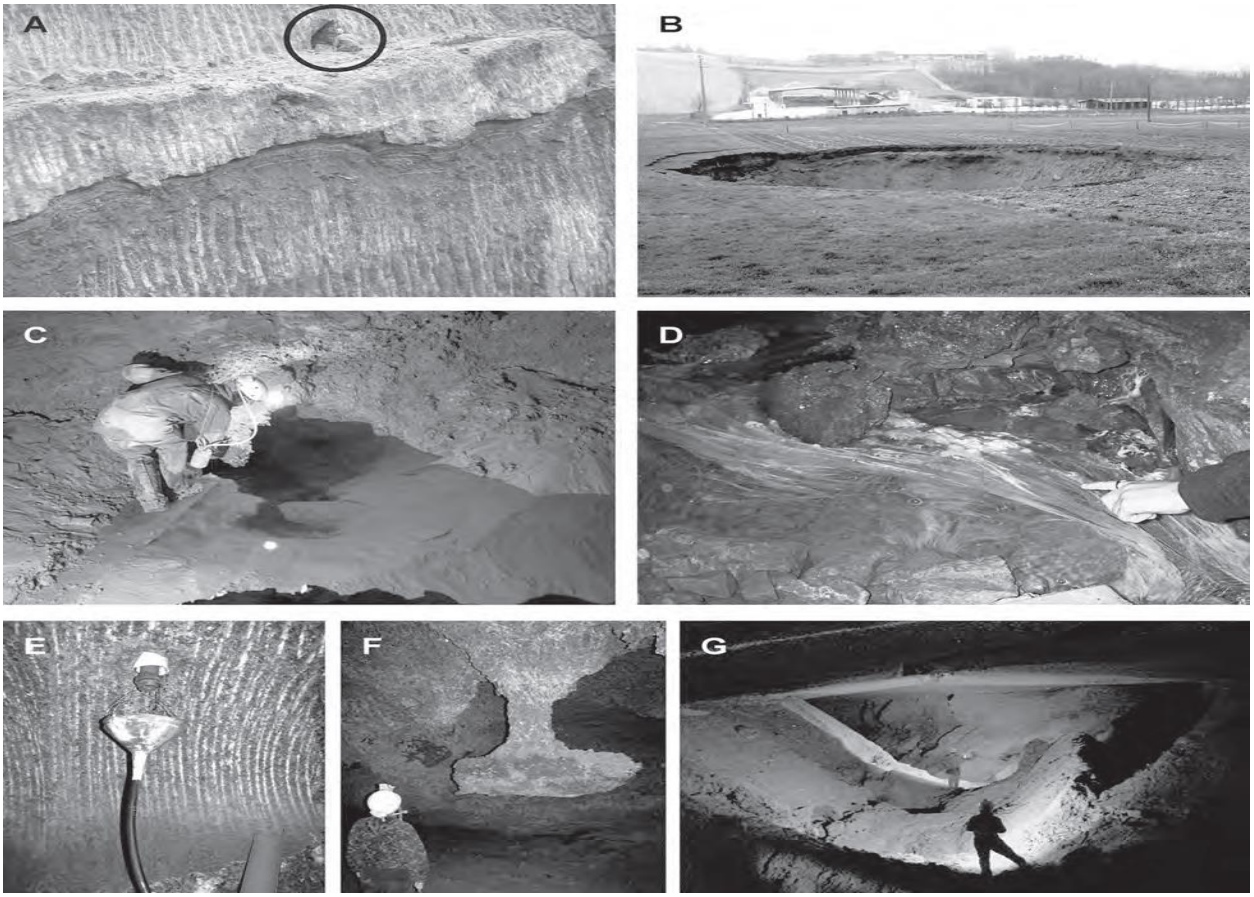

Figure 3 shows the sinkhole at Moncalvo, which was created when a karstic cave was intercepted on February 15, 2005, and collapsed into the underground quarry as a result. It also shows water upwelling from karstic conduits in the cave (VS), water rising from fissures with bacterial colonies (VB), and water rising from an open-air gypsum quarry with small intercepted caves (circle). gypsum pendant in the

Moncalvo cave; (F) intercepted in fissures in the quarry drifts (VC-VF); and (G) corrosion bevel in one of the caverns. (Conference paper January 2009, Messinian karst in Monferrato gypsum areas (North Italy) [8].

4) Geological and Geomorphological Observations

The gypsum deposit that is being exploited typically consists of massive macro- and microcrystalline beds that are 10 to 15 meters thick and are separated by marly interstrata that range in thickness from a few decimeters to a few meters (Fig. 3A). The bottom and top more or less impervious sediments (marls and clays of Tortonian and Messinian-Pliocene age, respectively) are sandwiched by this evaporite sequence. According to Klimchouk and Ford (2000), this constrained stratigraphic setting, which is typical of many gypsum deposits around the globe, can result in the development of an intrastratal karst where water is supplied from the nearby sediments both from above (epigenic) and below (hypogenic). In the case of Moncalvo, the karst system can be categorized as nearby and/or deeply seated because entrenchment of the surface drainage system has not fully dissected the gypsum formations (Klimchouk, 1996). These gypsum beds, which were previously submerged in the Late-Messinian sea and covered with the aforementioned impermeable clayey sediments, were exposed to meteoric agents in a continental environment for a relatively brief period of time before the end of the Messinian era. Gypsum dissolution has been observed, particularly in the uppermost evaporite beds, in the underground mines where the drifts have carved out tiny karst cavities. These caves are infrequently reachable by humans and, when they are, they have little growth. The same type of cavities can also be found in the northwest region of the adjacent underground excavations, at 150 m asl, as well as in the open-air Moncalvo quarry at an elevation of 190 m asl (Fig. 3A). All of these caverns appear to be restricted to the topmost layers, typically above or not far below the water table, and none of them seem to delve very deeply into the gypsum sequence (Fioraso et al., 2004). Rare fractures are found along the over 12 km of drifts in the Moncalvo underground quarry, and these occasionally transport minuscule amounts of water (Figs. 3C-D-E). The majority of these water-bearing cracks are found in the southeast corner of the quarry, between 129 and 150 meters above sea level. Mining activities have only led to the discovery of two significant caves. The caves have completely developed underwater, and they are typically distinguished by phreatic morphologies. There are no signs of speleothems, and the roof has a uniform surface with sporadic cupolas, morphs that resemble megascallops, ceiling pendants, and corrosion bevels (Fig. 3F) (Fig. 3G). Except for the final chamber in one of the caves, where material has come from the surface, the floor is covered with fine sediments derived from the marly interbeds (cover-collapse sinkhole). While mostly hidden by clayey sediments, several feeders can be seen in both caves in the shape of descending passages that indicate where rising water entered the cave (Fig. 3C). Because of breakdown, outlets are difficult to spot in some areas of the caves, nearest to the upper marl sequences (Vigna et al.,., 2009) [9].

1.2 QUARRY ACTIVITIES AND USE OF GYPSUM

1) ACTIVITIES CARRIED OUT IN QUARRY

The road header and personnel are moved about 5 meters higher, and the excavation is promptly stopped. The water discharge dramatically increases at 6 o'clock that day, and over the course of the following night, about 60,000 m3 of water bearing fine sediments are washed through the underground quarry and rise to a height of 139 m above sea level, partially engulfing the road header (Fig. 4). At the same time, a cover-collapse sinkhole that is 20 meters wide and 10 meters deep forms near to the NE edge of the quarry area (Fig. 5). A fracture is intercepted at a height of about 134 meters above sea level while a road header is excavating a drift that would have linked levels 1 and 2. This fracture released a small amount of water at a high hydraulic pressure (> 300,000 Pa) [10].

Figure 4 shows the drift before and after the sediment and water flow. Gypsum was being cut with a road header on February 15, 2005, just before the inrush; on February 16, 2005, the road header was nearly entirely covered by mud. On February 15, 2005, the water level stabilized at 139 meters above sea level.(Article in Zeitschrift für Geomorphologie Supplementary Issues · May 2010, Hypogene gypsum karst and sinkhole formation at Moncalvo (Asti, Italy).

A number of pumps were installed on February 23 to remove the water from the flooded passageways. A precise flow test made on April 15th yielded a result of 22.27 l/s. The water level gradually decreased over the course of the two months of draining, reaching 135.5 m asl on April 28th, allowing for a closer inspection of the inrush location. Continuous pumping has brought the water level down to below 134 meters above sea level, stabilizing the water flow from the captured karst at a rate of 20 liters per second. Cleaning the inrush point will take an additional three months, and it won't be until the end of July 2005 that the entry to the karstic cavity, from which the water rushed into the quarry during the inrush, will be visible [11].

Figure 5 shows three images of the cover-collapse sinkhole that resulted from the karst in the subterranean quarry being emptied and the karst voids' covering terrain collapsing.(Article in Zeitschrift für Geomorphologie Supplementary Issues · May 2010, Hypo gene gypsum karst and sinkhole formation at Moncalvo (Asti, Italy).

A number of continuously watched piezometers were in charge of controlling the hydrogeology of the underground quarry prior to the occurrence of karstic voids and sinkhole formation. Two boreholes located in the drifts have intercepted more significant water inlets showing hydraulic pressures of respectively 100,000 and 300,000 Pa in addition to the numerous small springs (typically less than 1 l/s) found along the drifts, particularly in the SE sector between 129 and 176 m a.s.l (1–3 bar). The virtual water table was stable at 170 meters above sea level before the incident, according to hydrological

measurements that have been repeatedly recorded. Hydraulic pressure must have been close to 360,000 Pa when the karst fissure was closed [12].

After the incident, the virtual water table dropped to 139 meters above sea level in just 14 hours, and by the end of 2005, less than 134 meters above sea level had been achieved due to constant pumping. The discharge has steadily declined since the event, peaking at slightly less than 10 l/s in the summer of 2005. Since then, it has remained largely stable, with only minor fluctuations (1-2 l/s) after heavy rainfalls (Fig. 6).A study of the primary elements and redox potential has been conducted as part of a monitoring program to describe the waters flowing in the gypsum discontinuities and in the karst systems (Eh) [13].

2) USE OF GYPSUM

Gypsum is increasingly in demand as a raw material in a variety of industrial sectors, including building engineering, medical applications, agriculture, the food industry, and the manufacture of paints. This implies that open pit and underground quarries all over the world are heavily exploiting this resource. According to the US Geological Survey on Mineral Commodity (February 2020), global mining operations used about 140 million tons of gypsum in 2019. A thorough understanding of the mechanical response of gypsum as a natural rock is required for the stability evaluation of these diffuse mining sites around the globe. Natural gypsum can have heterogeneous characteristics, even within a single rock facies, which makes mechanical characterization more difficult than with synthetic gypsum. The common practice of underground excavation frequently results in the omission of crucial information for the mechanical characterization of the ore deposits, to the detriment of both safety and productivity. This is because there isn't a clear focus on the relationship between gypsum geological variability and strength parameters. Additionally, there is a negative impact on the mechanical properties caused by the frequent presence of water or high humidity in underground drifts that, if ignored, could result in dangerous risk scenarios like roof collapses or pillar failure (Wang et al. 2008; Xia et al. 2019) [14].

PHYSICAL PROPERTIES OF GYPSUM [15]

Chemical Classification	Sulphate
Color	Clear, Colorless, White, Gray
Streak	White
Luster	Vitreous, Silky, Sugary
Diaphaneity	Transparent to Translucent
Cleavage	Perfect
Mohs Hardness	02
Specific Gravity	2.3
Diagnostic Properties	Cleavage, Specific Gravity, Low Hardness
Chemical Composition	Hydrous Calcium Sulphate
Crystal System	Monoclinic
Uses	Use to manufacture dry wall, plaster

3) GEOLOGY

In shallow coastal basins with arid to semi-arid climates and very little terrigenous siliciclastic sediment input from continental regions, gypsum deposits typically develop. Only during the Permian-Triassic in the Tethys basin (Stampfli et al., 2001) and the Messinian Salinity Crisis in the Mediterranean basin (Hsü et al., 1977; Roveri et al., 2001) did these circumstances exist in the Alpine and Apennine sedimentary sequences. While Messinian gypsum layers are interlayered with shaly sequences of marine environments, Permian-Triassic gypsum deposits are linked to peri-continental evaporite deposition, which also contains halite and dolomite deposits. Permian-Triassic evaporites are currently found primarily in the Eastern Alps and the Northern Apennines, while Messinian gypsum is found throughout the entire Apennine range, primarily in Sicily [16].

The different Uniaxial Compressive Strength Test performed in the past on gypsum had these results

Minimum : 4.6 MPa

Maximum : 25.2 MPa

Average : 13.6 MPa

4) GYPSUM'S APPLICATION

- Applications in architecture (wall board, plaster of Paris)
- Ground Screen (Gypsum Cement)
- Absorbents (ground management, drainage) (ground control, drainage)
- Decorative (Decorative stone, plaster sculptures) (Decorative stone, plaster castings)

Gypsum is primarily used in the production of wallboard and plasterboard, Portland cement, plaster of Paris, soil conditioning, and cement. Along with other goods like blackboard and sidewalk chalk, gypsum is also used to make fertilizer. Gypsum varieties known as "satin spar" and "alabaster" are used for a variety of ornamental uses, but their durability is constrained by their low hardness. The rock-like condition of gypsum can be restored by milling it with water. This means it can be molded and hardened. Additionally, because gypsum has a "closed recycling circle," it can be recycled indefinitely without losing any of its quality [17].

1.3 SCOPE OF THESIS

1) GYPSUM FORMATION AND EXPLOITATION

Gypsum is a crucial raw material for the building industry as well as other industries. Gypsum abuse has grown over the past few years as a result of the significant demand on the domestic and global markets. The Monferrato region of Piedmont is where the major gypsum bodies are found. The outcrops of gypsum-bearing formations exhibit typical geological, structural, and hydrogeological characteristics that may affect quarrying utilization. In light of a recent new hypothesis regarding the geological and structural setting of the gypsum deposits in the Monferrato area, special consideration will be given to how these hypotheses may affect conventional surveying techniques, while also taking into account geo-mechanical factors associated with the presence of karst phenomena and stratigraphical or structural marly layers [18].

In the last few years, there has been a rise in the number of people using the internet to buy goods and services. Like with all natural resources, improper handling of gypsum extraction has frequently led to issues with the environment and public safety that are related to the stability of the drift and the risk of subsidence on the surface, as well as the quarry face. For that reason, both geo-mechanical behaviour and geo-hydrological features of the gypsum deposit have to be precisely specified to program \ssuitable surveys, planning and management of the quarry. The majority of Piedmont's exploited gypsum bodies are part of the Messinian "Formazione Gessoso Solfifera" (also known as the "Complesso Caotico di Valle Versa"; Dela Pierre et al., 2003), and they are distributed along two broad bands that border the Tertiary Piedmont Basin to the north and south. The north belt runs in a discontinuous fashion for 35 kilometers, from Moncucco to Ottiglio (Monferrato domain), while the south belt (Langhe domain) runs for almost 25 km crossing the \swhole central region of Piedmont from W to E (Fig. 6) [19].

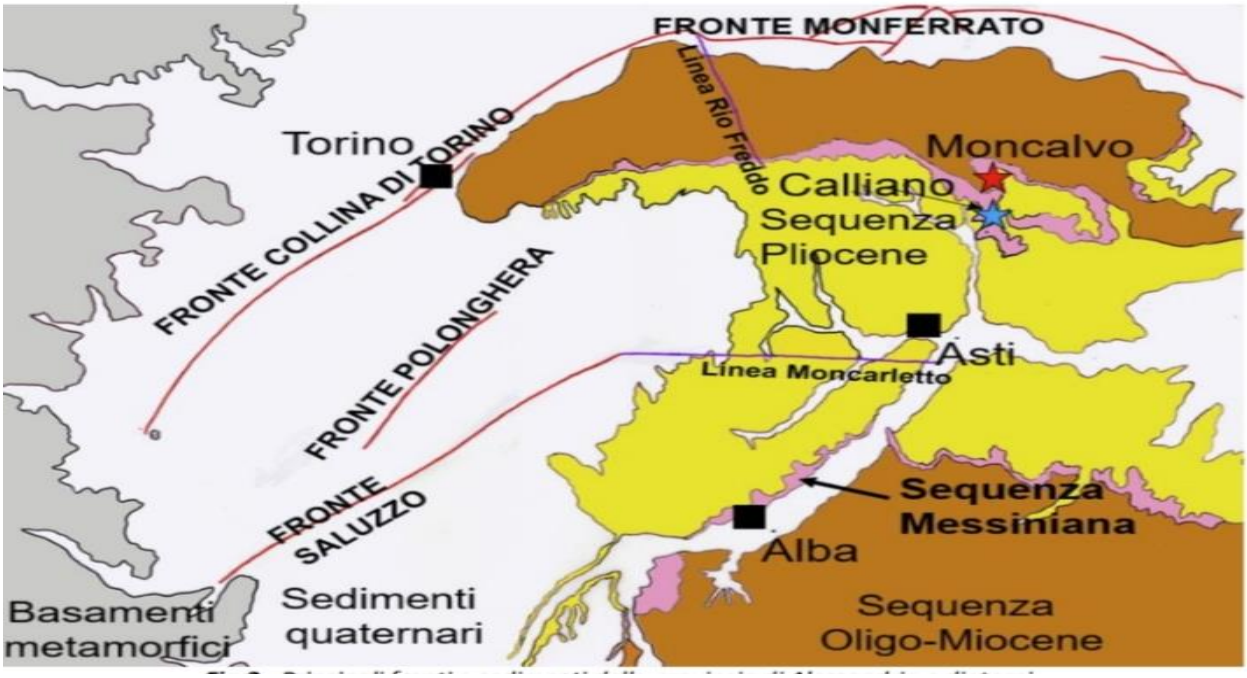

Figure 6 shows a geological diagram of the Tertiary Piedmont Basin; the Messinian formation's rocks are shown in black.

There were numerous open pit and underground quarries in those regions, the majority of which had been abandoned; currently, only four gypsum quarries in the Monferrato domain are still in operation [20].

2) Local Properties of Formation on a Macro and Micro Scale

The "Formazione Gessoso Solfifera" (Messian) can have a total thickness of up to 400 meters, but the thickness of the gypsum masses that are included varies greatly and is occasionally difficult to gauge. While it rarely exceeds 20 to 30 meters in the south belt, they frequently seem to reach 60 to 70 meters in the north belt. (with values increasing going from West to East). The messinian succession is characterized by cycles composed of pre-evaporitic deposits - made of thin sands, silts and laminated clays - evaporitic beds - mainly composed of a basal carbonate level and layers of gypsum separated by marls and algal carbonates - and post-evaporitic sediments, consisting of grey marls, needle-shaped gypsum crystals, clays and local conglomerates (Bonsignore et al., 1969; Sturani, 1976). The locations of the original basin's deposition sites and later tectonic events determine the thickness and presence of the various types of deposits. Gypsum formations have traditionally been thought of as lenses with a total length of hundreds of meters, made up of interbedded layers of marls that range in thickness from a few decimeters to several meters. Gypsum beds display two facies with distinct mechanical and industrial properties: a small-grained selenitic facies with crystal sizes varying from a few millimeters to several centimeters, and a coarse-granulated facies with grain sizes up to tens of centimeters. Locally, tectonic discontinuities that are occasionally exposed and refilled with marls and clays are also interesting to

gypsum lenses. Based on the field evidence gathered, this geological model does not adequately explain the local environment in some places. As a matter of fact, somewhere (as for exemple in the Montiglio and Moncucco area), gypsum bodies seem to belong to a chaotic deposit resting unconformably on the older geological formations and interpreted as a melange of different blocks (made of bioclastic rudstones, coquinoid grainstones, limestone, dolomite, carbonate monogenic breccias, conglomerates, marls and gypsum) floating in a matrix of weakly consolidated “mud breccias”. In particular, the matrix is made up of deposits that are brownish silty-marly and that contain tiny clasts of grey marl that range in size from a few millimeters to several centimeters. The "melange" most likely results from gravity-driven processes and mud diapirism phenomena (indicated by carbonate made of methane), both of which are connected to tectonic movements. This theory holds that gypsum bodies are irregular slabs with a range of sizes, from a few meters to several hundred meters in length and a few meters in thickness. They mostly preserve the usual depositional succession of alternating coarse- and fine-grained gypsum beds and marly layers, but there are also more clastic gypsum facies and tectonic structures with marly-clay refilling [21].

Figure 7 Formations of Moncalvo Quarry.(Moncalvo Site visit 2023) [22].

Gypsum bodies' shapes and their initial stratigraphic relationships with neighboring deposits are occasionally unclear because of genesis mechanisms. Because tectonic contacts fully encircle each block, lateral continuity is not guaranteed. In order to determine the size, shape, orientation, structure, and thickness of the overburden deposits, more consideration must be given to the choice and accuracy of surveying techniques. Due to their impact on the management of the quarrying activity starting at the planning stage, all of these parameters must be precisely identified in order to succeed in the exploitation activity. In addition to field observations, drillings and, ultimately, geophysical surveys using electrical techniques (SEV or electric tomography) and seismic refraction methodology are typically used to reconstruct the geological setting. Drilling must increase and geophysical studies are required due to the deposits' potentially chaotic setup. Since the geological environment is so unpredictable, isolated drillings can only provide partial information, and straightforward correlations between them are unreliable. Additionally, drilling enables the execution of in-situ tests as well as the collection of samples for laboratory and analytical testing in order to determine the gypsum quality and geotechnical parameters of

exploited deposits and overburdens. (cohesion, angle of repose, specific weight, deformation modulus, elasticity modulus, section modulus, compressive strength, shear strength). Due to the short number and limited size of outcropping areas, when open pit or underground quarries are already present, structural setting as well as physical, mechanical and hydraulic features of discontinuities can be appropriately investigated by means of detailed structural surveys in correspondence of existing quarry faces and drifts [23].

3) Description of Typical and Challenging Phenomena with Water Interference

Due to the existence of faults, open fractures, and karst voids, gypsum bodies can be compared to bedrock aquifer systems due to their poor primary permeability and geo-structural characteristics.Open discontinuities are both a path for this water to leak out and a pathway for water that will ultimately flow from the bottom. Infiltration and diffusion phenomena through the overburden represent a way for water to inflow from the surface. Due to its high solubility, one of the major issues with gypsum extraction is the existence of active karst or the presence of abandoned karst voids that have been filled with leftover deposits. (usually clay and marls). Gypsum karst has a big effect on quarrying, and quarrying can have a big impact on gypsum karst as well, especially when changes in groundwater circulation are caused and the quarry interferes with the local hydrogeological setting. Exploitation activities may result in hazardous water inrushes, depletion of natural water resources, and a decline in the water table in communicating surface areas if proper quarrying management and a consistent geo-survey are not implemented [24].

Aquifers, accelerated water flow and gypsum dissolution, collapses, and expansion of drawdown cones. In some instances, gravitational breakdowns can start in the karst unit and then progress upward through the beds above it until they reach the surface and cause subsidence phenomena. (Fig.8).

Figure 8 shows the sinkhole that has appeared in the Moncalvo gypsum quarry region. (Geo-surveying for safe underground mining in gypsum deposit in Monferrato basin (Italy) / BONETTO S; FORNARO M; OGGERI C.. - (2006), pp. 382-387. ((Intervento presentato al convegno MPES2006 tenutosi a Turin nel 20-22 Sept.2006) [25].

Gypsum karsts start to form in deep-seated environments and continue to change as gypsum layers are uplifted into shallower positions as a result of tectonic events and the input of erosional activity.

Such growth frequently takes place in restricted hydrogeological settings before evolving into phreatic and vadose settings. Depending on the original pattern of discontinuities, under confined circumstances, Phreatic and vadose conditions, on the other hand, favor the development of linear or dendritic tunnel systems. Active groundwater circulation favors the development of uniform maze conduit systems or solitary large voids. Actually, the upper portion of the gypsum body, especially up to the talweg of the major local river, has been where evidence of dissolution processes and karst activity in gypsum deposits has been most prominently seen. (Fioraso & Boano, 2002) Since discontinuities and karst system characteristics directly affect how water circulates in gypsum bodies, structural setting of the deposits and voids distribution must be determined as exactly as possible using geo-mechanic surveys and geophysical techniques. Data collected during geo-mechanic surveys display orientation and extension of main discontinuity systems and, consequently, hypothetical water flow directions; besides, opening and frequency features of discontinuities furnish average permeability values for gypsum body, for example using Snow (1969) or Kiraly-Louis (1969) equations. Lugeon Tests can also be used to study permeability conditions, but their accuracy is heavily dependent on how the test is conducted and the precise geostructural environment. Finally, results from Lugeon Tests and geomechanic surveys can be contrasted [26].

In order to examine the presence of water in the various sectors of the exploited area, some piezometers must be planned based on the hydrogeological behavior of gypsum bodies. Additionally, tracer tests can be performed using fluorescent tracer introduced in properly drilled boreholes, monitoring its presence in piezometers situated outside of the exploited area, to confirm the existence of connections between water inside and outside the quarry. When it comes to geophysical surveys, the most significant findings have been made by combining electrical and seismic refraction methodology with strategically placed drillings to set the geophysical data gathered. Thus, it is feasible to highlight the existence of faults, shear zones, karst caves, and burden thickness in the gypsum body, for example. (Ferrero et al, 1990). Testing periodically small portions of the deposit or even individual exploitation panels can improve the reliability of the data processed; however, this solution takes time and a sizable amount of liquid assets.

Horizontal drillings can be occasionally renewed during quarry face exploitation in order to take precautions and stop water inrushes caused by the unexpected presence of active karst circuits. This will also make it possible to update and ultimately revise project data and geological information. Installing a suitable drain cock with a manometer is advised in the event of water inflow through the drillings in order to watch the water pressure behind the quarry face and prevent an uncontrolled water inrush [27].

In subterranean quarries, inflowing water is gathered in designated basins and pumped outside. During quarrying operations, systematic pumping is acceptable, but it cannot last for an extended period of time during the restoration phase. Because of this, whenever feasible, a new flow path needs to be established to reintroduce water into natural circuits, such as through the use of gravity drains or pipes [28].

1.4 SURVEY AND MONITERING

1) SURVEYING AND MONITERING METHODOLOGIES

The karst tunnel behind the mining face was scoured due to the water level in the drift decreasing. Three major linked conduits and a sizable room (a few hundred cubic meters) that were pointed in the directions of SO, NW, and NNW, respectively, were also found. (Fig. 09) [29].

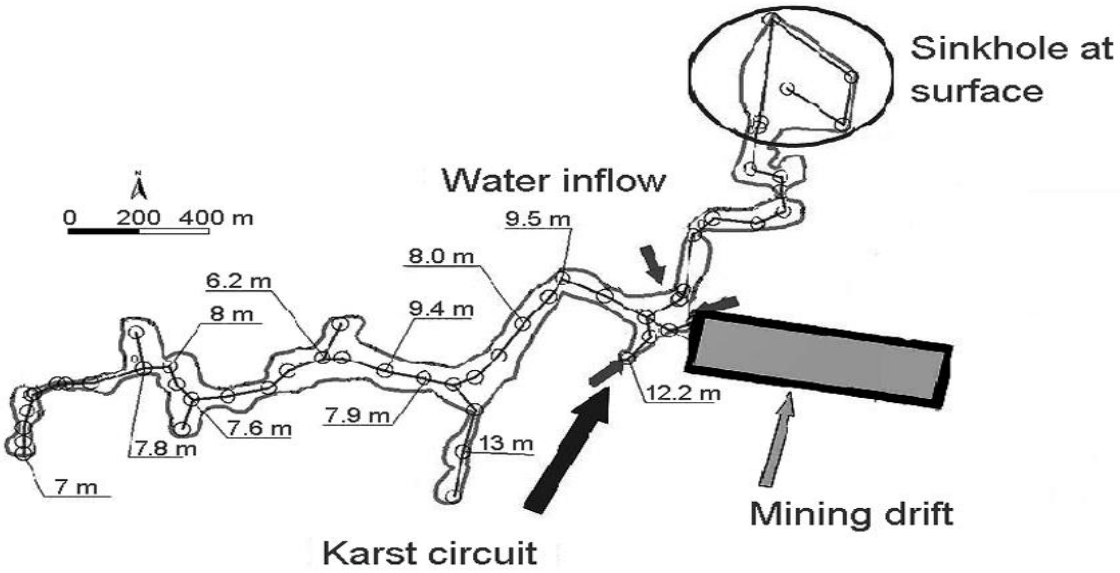

Figure 9 Diagram of the investigated karst circuits following the inrush event's lowering of the water level.(Article in Estonian Journal of Earth Sciences · September 2008) [30].

The 10 m-long southwesterly conduit connects to a siphon where the primary water inflow begins. The second pipe has a circular diameter of roughly 57 m and continues for about 200 m to the northwest along the marly layer between the second and third strata of coarse-grained gypsum. (Fig.10).The distance between the roof of the cave and the bottom of the drift ranges from 6 to 13 meters. It is situated directly beneath the quarry drifts. The cave's dome roof provides assurance about the stability of the voids and indicates that it was a conduit carrying a heavy load. The third conduit, which has an irregular section and is about 100 meters long, travels through the three levels of coarse-grained gypsum. In reality, it terminates at a sinkhole with a funnel-shaped deposit of terrigenous sediments and woody material that came from the surface. The major water inflow came from the siphon of the southwestward conduit, while the other one was linked to a discontinuity and revealed a discharge of a few liters per second during scouring operations in the large room immediately behind the mining face. In addition to safety

restoration efforts, surface and subsurface research was done to better understand groundwater circulation, the causes of the sinkhole occurrence, and the source and quality of water inflows [31].

Three borings (SN1, SN2, and S24) and the geophysical technique, which makes use of electrical and seismic refraction tomography, were used to perform subsurface exploration, which made it possible to

Figure 10 shows an illustration of pipelines and rooms found during the speleological surveying.(Article in Estonian Journal of Earth Sciences · September 2008) [32].

Reassemble the geology and overburden layers of the area. To track the groundwater table in connection to rainfall and mine water pumping, boreholes were fitted with piezometers and an automatic rain gauge (with hourly measurements). Chemical and physical laboratory tests were used to gather and analyze the water inflows in the karst conduits (VS, VB, and VR) and the quarry (VC, VP3, VBA, and VBB) on a seasonal basis. The level, temperature, and electrical conductivity of the water coming from the karst system were also measured using a weir that had a digital data-logger installed close to the site of the inrush. (Fig. 11) [33]

The discharge values recorded at the weir have remained relatively constant for over a year (around 10 l/s), with a slight increase of about 1/2 l/s during significant rainfall events (February 2006, May 2006, September 2006, and May 2007; Fig. 12). In a similar vein, data collected have shown a strong correlation between water pumping in the quarry and piezometric measurements, but no correlation has been found between groundwater table levels in piezometers and rainfall; all values seem to be independent of one another and different from the value directly monitored in the drifts (SN1 = 214 m

a.s.l.; SN2 = 184.3 m a.s.l.; S4 = 225 m a.s.l. Without taking into account discharge variations, the temperature values measured in the weir are also nearly constant with a slight variation of 0.5 °C. primarily follows stratigraphical discontinuities and fissures, such as the contacts between gypsum strata and marl layers. One of the major scoured pipelines actually forms at the base of the second coarse-grained gypsum stratum, right where it meets the marly layer below. The existence of small karst caves at the interface between the Messinian evaporitic formation (Gessoso Solfifera Formation) and the older Tortonian marls (Sant'Agata Fossile Formation) was discovered by drilling, along with other similar evi

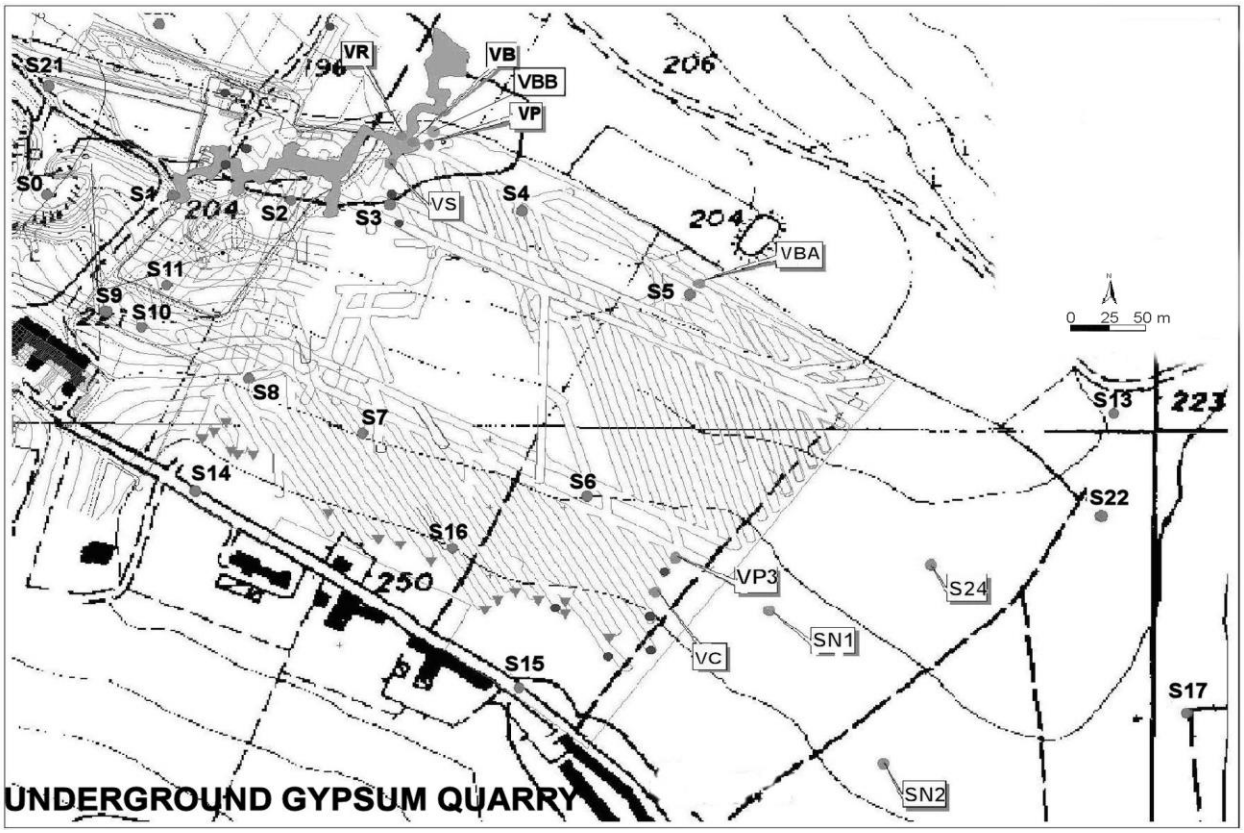

Figure 11 shows the distribution of the monitoring sites (water inflows: VC, VB, VR, VS, VP, VP3, VBA, VBB; old drillings: SOS11, S13S17, S21S23; new drillings with piezometers: SN1, SN2, S24).(Article in Estonian Journal of Earth Sciences · September 2008) [34].

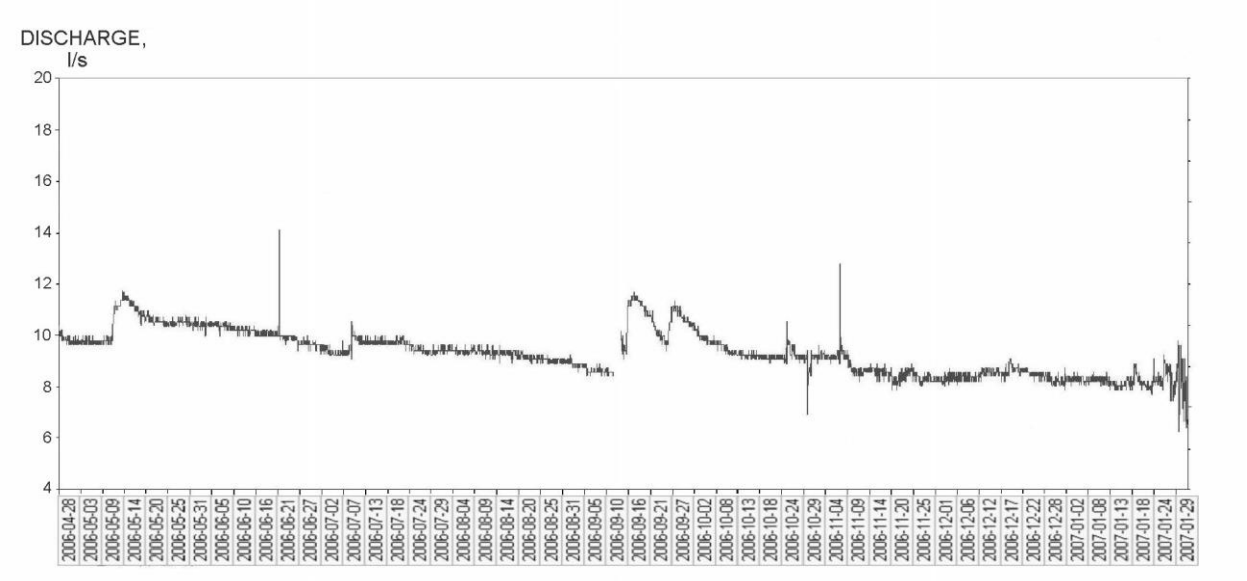

Figure 12 shows the inrush flow trend as observed at the weir. (Article in Estonian Journal of Earth Sciences · September 2008) [35].

1.5 THE GEOLOGICAL STRENGTH INDEX (GSI)

In order to provide accurate rock mass characterization for engineering rock mechanics, the Geological Strength Index (GSI) method was created. For designing tunnels, slopes, or foundations in rocks, numerical analysis or closed-form solutions need raw data pertaining to the properties of the rock bulk. The selection of parameters for predicting the strength and deformability of rock masses is directly influenced by the geological characteristics of the rock material and a visual evaluation of the mass it creates. By using this method, it is possible to think of a granite mass as a mechanical continuum without losing sight of the impact that geology has on its mechanical characteristics. Additionally, it offers a field technique for describing challenging rock formations. The tunnel designer can now analyze progressive failure processes using numerical tools, as well as the sequentially installed reinforcement and support required to keep the stability of the advancing tunnel until the final reinforcing or supporting structure can be installed. These numerical tools need accurate input data on the tensile and deformation properties of the rock bulk encircling the tunnel, though. With the exception of back analysis of tunnels that have already been built, it is practically impossible to ascertain this information through direct in situ testing, so there is a greater need for estimating the properties of the rock mass from the intact rock properties and the characteristics of the rock mass discontinuities. Hoek and Brown [1980] created the rock mass failure criterion as a consequence of this [36]

1) GEOLOGICAL STRENGTH INDEX FUNCTIONS

The meticulous engineering geology description of the rock mass, which is primarily qualitative and forms the basis of the GSI classification, is at its core. For weak and complex rock masses, on joints were

essentially meaningless. Since the GSI system lacks the ability to design supports or reinforce rock masses, it should be noted that it was never meant to replace RMR or Q. The only purpose of the GSI is to estimate the properties of the rock mass; it is not an instrument for tunnel construction. It should never be used separately of the intact rock strength because they are inextricably linked.

This index is calculated from visual inspection of the rock mass exposed in outcrops, surface excavations like road cuts, tunnel faces, and borehole cores. It is based on an assessment of the lithology, structure, and condition of discontinuity surfaces in the rock mass. The GSI observes the primary geological constraints that control a formation by combining the two fundamental geological process parameters—the blockiness of the mass and the conditions of discontinuities. Thus, it is a reliable geological indicator that is easy to use in the field.

Note that while efforts to "quantify" the GSI classification [Cai et al. 2004; Sonmez and Ulusay 1999] are fascinating, they must be used with care to avoid losing the geologic logic of the GSI system. This is because it is believed that "engineers are happier with numbers." The quantification methods are limited to rock masses in which these numbers can be readily measured and are linked to the frequency and orientation of discontinuities. In tectonically disturbed rock formations where the structural fabric has been destroyed, these quantifications do not perform well. The authors advise using the original qualitative method based on meticulous visual observations in such rock masses. The "quantification" system is only applicable, say, in the range of 35 to 75 GSI, when the behavior of the rock mass depends on the sliding and rotation of intact rock pieces and the spacing and condition of the discontinuities that separate these pieces, rather than the intact rock strength, determine the behavior. The measurement is no longer accurate if the whole rock fragments can fracture [37].

2) GSI Chart's geological description

The choice of the suitable case in the GSI chart for dealing with particular rock masses is advised not to be restricted to the visual similarity with the sketches of the rock mass's structure as they appear in the charts. To select the most appropriate structure, it is also necessary to thoroughly read the associated descriptions. The most appropriate instance might be somewhere in the middle of the charts' sparse collection of sketches or descriptions [38].

3) GSI Values Projected Into the Ground

The most typical sources of information for calculating the GSI value of a granite mass are outcrops, excavated slopes, tunnel faces, and borehole cores. What projection or extrapolation should be made of the figures approximated from these sources into the rock mass behind a slope or in front of a passage? In the early phases of a project, outcrops are a very valuable source of data, but they have the drawback that surface relaxation, weathering, and/or alteration may have significantly changed the appearance of the rock mass components. Trial trenches can be used to avoid this drawback, but there is no assurance that the effects of deep weathering will have been eliminated unless these are machine-excavated to a significant depth. Therefore, judgment is needed to account for these weathering and alteration effects when determining the most likely GSI value at the suggested excavation's depth. These faces are probably the most reliable sources of information for GSI estimates because they are situated relatively near to and

within the same rock mass as the excavation under investigation. A borehole core is the best source of information at deep, but it is important to realize that the one-dimensional information from the core must be extrapolated to the three-dimensional in situ rock mass. The majority of knowledgeable engineering geologists are acclimated to using this extrapolation method, but this is a problem that affects all borehole investigations. The evaluation for a slope's stability analysis is based on the mass of rock through which it is thought that a potential failure plane might travel. In these situations, estimating the GSI values takes a great deal of discretion, especially when the failure plane can pass through several zones of varying quality. In this situation, mean values might not be suitable. The index for tunnel behavior should be evaluated for the volume of rock engaged in carrying loads, such as for a structure like the elephant foot of a steel arch, or more locally in the case of a tunnel. In a broader sense, the numerical models might take into account the variation in GSI values over the passage in [39].

4) The Discontinuities' Aperture

The interlocking of the individual intact rock fragments that make up a rock mass determines the mass's strength and deformation traits. Clearly, the aperture of the discontinuities that divide these parts has a significant impact on the properties of the rock bulk. A "disturbance factor" D has been provided in the most recent Hoek-Brown failure criterion [Hoek et al. 2002] and is also used in the Hoek and Diederichs [2006] approach for estimating deformation modulus, though there is no specific mention of the aperture of the discontinuities in the GSI chart. This factor varies from D=0 for completely undisturbed rock masses, like those excavated by a tunnel boring machine, to D=1 for completely disturbed rock masses, like open-pit mine slopes that have undergone extremely heavy production blasting. The component permits the opening of the discontinuities, which prevents the individual rock fragments from interlocking. This factor's impact on the computed safety factors is extremely important. As more field evidence is gathered, it may be necessary to modify this factor's participation in the equations because there is currently comparatively little experience using it. But based on the experience to date, it appears that this component does offer a reliable approximation of the impact of damage from stress relaxation or blasting of excavated rock faces. Noting that this damage decreases with depth into the rock mass, it is usually appropriate to simulate this decline in numerical modeling by dividing the rock mass into a number of zones and applying progressively decreasing values of D to each zone as the distance from the face increases. Regarding the severity of this damage and how it affects the properties of rock mass, Hoek and Karzulovic [2000] have provided some advice. The blast damage is typically milder in severity and scope for civil engineering slopes or foundation excavation, and the value of D is low. Since excavation is typically done using "gentle" mechanical methods and the amount of surface damage is minimal compared to that which already exists in the rock mass, this issue becomes less significant in weak and tectonically disturbed rock masses [40].

5) Great Depth Geological Strength Index

The tightness of the rock mass structure in hard rock at large depths (i.e., 1,000 m or more) causes the mass behavior to resemble that of the intact rock. The GSI value in this situation is getting close to 100, and the GSI system program is no longer useful.

Under these circumstances, brittle fracture initiation and propagation dominate the failure process that determines the stability of underground excavations, which can result in rock bursts, slabbing, spalling, and other problems.

The study of these brittle fracture processes has received significant research attention; Dietrich's et al. [2004] provide an insightful overview of this work. These remarks do not apply when tectonic disturbance is significant and persists with depth, and the GSI charts may be used instead [41].

6) Effects of Water

When filling materials or discontinuities contain water and are susceptible to deterioration due to variations in moisture content, the shear strength of the rock mass is decreased. This is especially true for the "fair" to "very poor" groups of discontinuities, where wet circumstances may cause a shift to the right. When the quality of the rock bulk is lower, there is a more noticeable shift to the right. (last rows and columns of the chart). Effective stress analysis is used to cope with water pressure during design, and it is autonomous of the GSI characterization of the rock mass [42].

7) THE GSI CLASSIFICATION SYSTEM'S PRECISION

For engineering geologists, the "qualitative" GSI method works well because it is congruent with how they have previously described rocks and rock masses during logging and mapping. Engineers sometimes have a hard time using the system because it lacks parameters that could be measured to increase the accuracy of the predicted GSI value. The writers disagree with this worry because they think it is pointless to try to calculate the exact value of the GSI for a typical rock mass. In all but the most straightforward of circumstances, it is best to characterize GSI by giving it a range of values. This region may be described analytically by a normal distribution with mean and standard deviation. GSI is a completely independent system, but during the early stages of its implementation, it was suggested that

Correlation of "adjusted" RMR and Q readings with GSI can be used to supply the Hoek-Brown criterion with the data it needs. Although this method might be effective with rock masses of higher grade, it is unreliable with weak, very weak, and heterogeneous rock masses, where these correlations are not advised (for example, GSI35). Every time GSI is used, a straight evaluation based on the tenets and graphs shown above is advised. Thankfully, the majority of GSI users have no trouble considering it to be an entirely separate system. A shared fabric index chart groups the ratings of all four classification-characterization systems (RMR, Q, RMi [Palmström 1996], and GSI) together. The reader is advised to keep in mind the actual geological world when thinking about such connections [43].

CHAPTER 02

2.1 MONCALVO QUARRY

1) The Moncalvo d'Asti Caverns

In the Monferrato hills, surface expression of gypsum bodies is uncommon; access is given by both open-pit and underground mines. Two closely spaced quarries near the Moncalvo town have made it possible to explore gypsum caverns. A succession of shallow sinkholes with steep walls that can reach a depth of 10 meters have been encountered during the excavation of the gypsum beds in the first open-pit quarry, the majority of which have been completely filled in by silty-clayey deposits. The second quarry is underground and has over 20 km of tunnels. In 2005, as tunnels were being built to access the second macro crystalline gypsum bed, an entirely water-filled cave was discovered at the excavation front (Fig. 13). Due to this, a flood of water and mud with a flow rate of several m3/s inundated the quarry's lowest level (Vigna et al. 2008, 2010a, b). Moncalvo 1 and 2, two cave sectors that were discovered through subsequent speleological investigations, are divided by a short passageway filled with sediment. While the second sector (Moncalvo 2) is 480 m long and 30 m deep, the first one (Moncalvo 1) has a total development of 370 m and a positive altitude differential of 30 m [44].

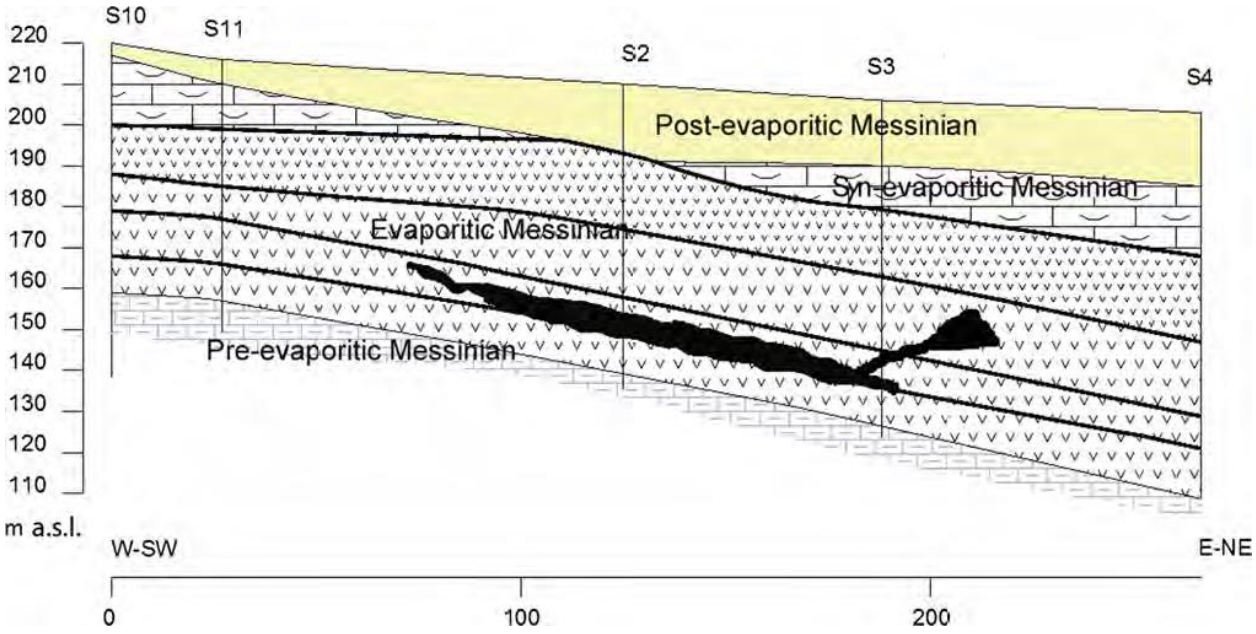

Figure 13 The Moncalvo cave system, which was formed between the first and second gypsum beds, is depicted in sketch outline. (Hypogene Gypsum Caves in Piedmont (N-Italy) Chapter · August 2017).

The first and second macro crystalline gypsum beds are separated by a layer of 1 m of finely laminated clayey-marly sediments, and both sectors are a component of a single system (Fig. 14) of phreatic conduits that developed along this layer. A secondary branch of the Moncalvo 1 sector (Fig. 15), which extends for about 100 m and traverses all three gypsum beds, comes to rest next to a sinkhole that appeared at the surface directly after the water inrush and is surrounded by a large collapse room. The main cave branch, which grows in a NW direction, is distinguished by a roughly cylindrical passageway that is 4-6 meters wide. Large pendants that occasionally split the passage are common (Fig. 16), and the floor, which is littered with debris and marly blocks, is encrusted with a channel created when the passages were quickly drained right after the mining works intercepted the cave. The farthest reaches of the cave are blocked by sediments that prohibit exploration of other areas of the cave system. A second, 20-meter-long branch that leads to the second sector of the tunnel (Moncalvo 2) is similarly blocked by sediments. On the left side of the cave's entry, a short descending conduit measuring 10 meters long could be seen. It came to a stop in a small sump where the water flow originated. To enable the secure removal of gypsum from the lower floors, a further artificial lowering of the water level was carried out in February 2010. The thin carbonate layer that is present at the foot of the evaporite sequence has been intercepted by a few boreholes that were dug in the quarry's lowest parts. The majority of the water from the mine has been drained by this heavily karstified limestone bed. A small opening at the excavation front of the second level of the underground quarry provides entry to the second sector of the cave (Moncalvo 2). This doorway leads to a narrow passageway that is 1.5–2 meters height. Immediately noticeable phreatic morphologies include a number of cupolas produced by upward flow (Fig. 17). After 30 meters, a major split is discovered: upward, a narrow passage (0.7–0.8 m) provides access to a wide passage (Branch of the Flat Ceiling), which will be described later, while downward, the conduit of varying sizes continues with an alternation of narrowings and wider parts, as well as some rising shafts that perforate the above-lying marly layer that divides the various gypsum beds. The marly layer above is frequently reached by the complete downstream branch, which is carved into the topmost portion of the gypsum bed. There are numerous secondary inlets to the main conduit, each of which has a few meters of impassable narrow phreatic tunnels. Moncalvo 2's final sections consist of a number of tight passageways that link small rooms with large gypsum crystals up to 1 m in length. These passageways are partially blocked with sediments. These crystals, which were precipitated from oversaturated waters, have developed in the marly interbed's fissures. In this area, the rapid dewatering of the tunnel passage caused collapse, leaving broken gypsum crystals on the floor. At 200 meters from the entrance, marly debris blocks the path. Due to its proximity to Moncalvo 1 sector—only 4 meters away—this passage has a powerful airflow [45].

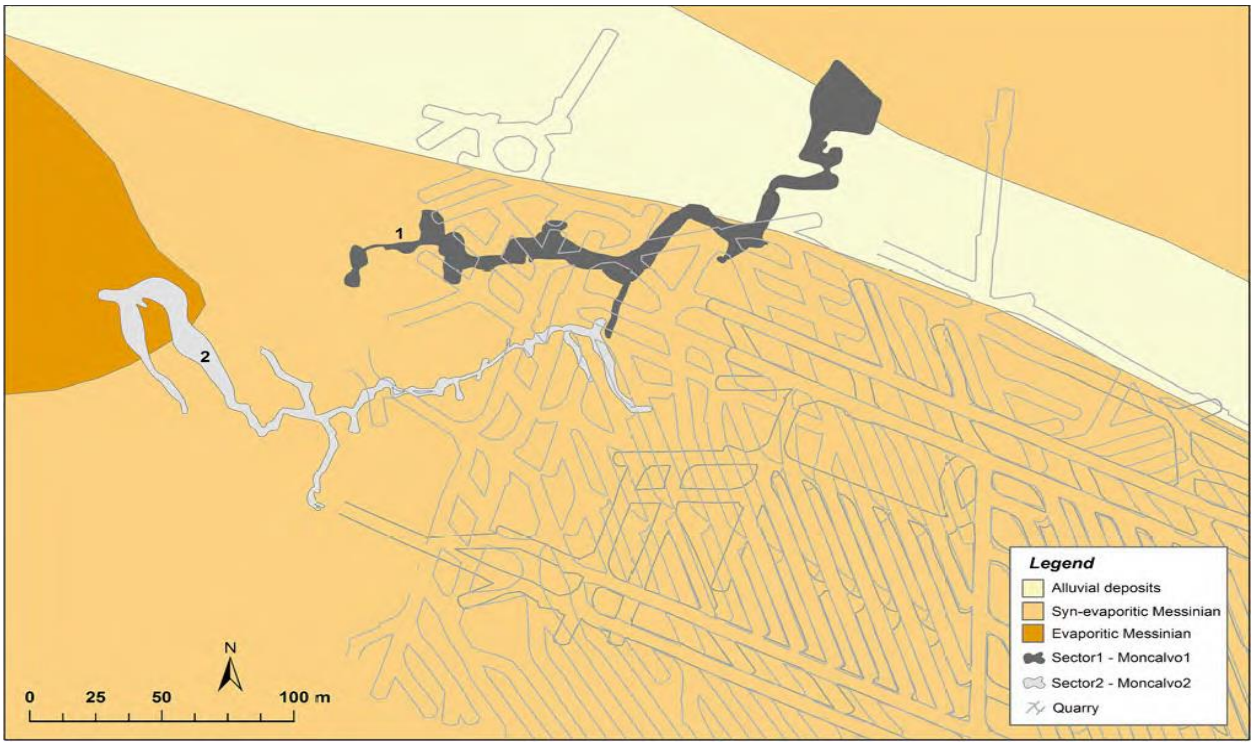

Figure 14 Moncalvo Tunnel system.(Hypogene Gypsum Caves in Piedmont (N-Italy) Chapter · August 2017) [46].

Figure 15 Typical phreatic morphology of the Moncalvo cave passageways(Hypogene Gypsum Caves in Piedmont (N-Italy) Chapter · August 2017).

Figure 16 Monclavo: Gypsum pendants on the cave's roof separate its passageway.(Hypogene Gypsum Caves in Piedmont (N-Italy) Chapter · August 2017) [47].

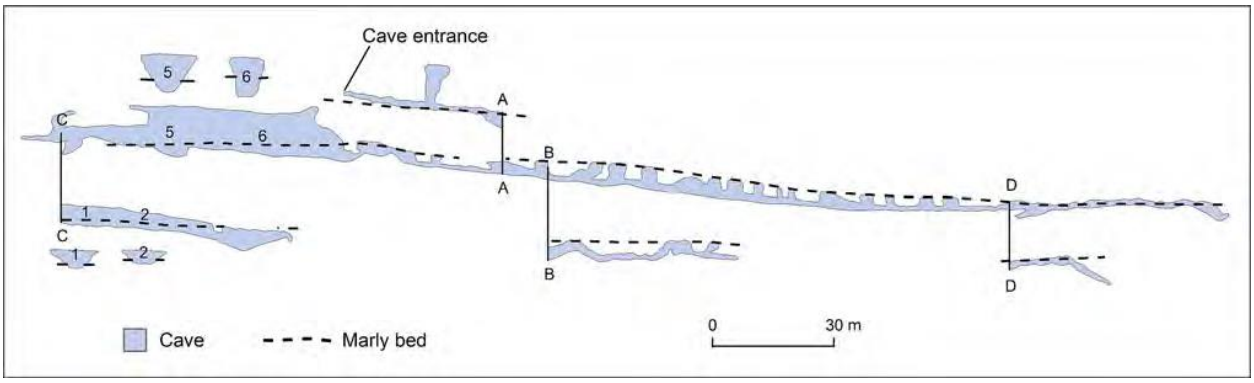

Figure 17 shows the longitudinal profile of Moncalvo Cave 2, which develops on the top edge of the first gypsum bed and has a number of partially carved ceiling cupolas.(Hypogene Gypsum Caves in Piedmont (N-Italy) Chapter · August 2017).

The 150 m-long Branch of the Flat Ceiling is distinguished by a very wide passage that is between 5 and 10 meters in height and 5 to 10 meters in width. The ceiling is perfectly flat and carved with tiny vertical fractures that have been expanded by descending infiltration water at the distal end of the upstream section (Fig. 18). The highest point the water table appears to have reached before the caverns were blocked by the underground quarry appears to be defined by this flat ceiling. This ceiling's elevation is a

perfect fit for the water level that was detected in the quarry's two piezometers just prior to the water inrush. The complete cave network forms between 20 and 60 meters below the surface of the earth.

Figure 18 Moncalvo shows how a stationary water table level before the underground quarry's interception caused a flat ceiling with a tiny ceiling channel.(Hypogene Gypsum Caves in Piedmont (N-Italy) Chapter · August 2017) [48].

2) Subsurface Water Science

A geochemical analysis of the groundwater in the Moncalvo region was carried out after the water inrush of 2005.Multiparametric sensors were placed, flow rates were monitored, and various waters in this karst system (from caves, fractures in the quarry galleries, and boreholes) were chemically analyzed. All of the waters circulating in the gypsum aquifer are of the calcium-sulfate facies from a geochemical perspective, but there are some variations between the waters based on flow paths through the aquifer and their origin.These waters' nitrate content (NO_3) and redox potential (Eh) have enabled for chemical differentiation. Local infiltration water (LIW) samples in Fig. 19 are surface waters that have a very positive redox potential and high nitrate concentrations (often surpassing 20 mg/L). After passing through the above-lying silty-clayey deposits, these waters, which are slightly undersaturated in gypsum, come into touch with the gypsum rocks. Between the gypsum rocks and the overlying sediments, these fluids frequently form vertical shafts. Other water samples taken from evaporite rock fissures have negative redox potential ("deep circulation water"; DCW samples in Fig. 19), low nitrate concentrations that are frequently below detection limit (0.01 mg/L), and are supersaturated with gypsum. These waters flow in the underlying fractured marly rocks (Marls of S. Agata Fossili), below the described evaporitic sequence, and should be significantly undersaturated in gypsum. Their temperature is comparable to that running in

karst systems (slightly higher). Some springs flowing out of the Pre-Messinian successions near to Moncalvo have also been discovered to have water with similar characteristics (negative redox potentials, absence of nitrates, and strongly undersaturated gypsum). These liquids have a potent potential for dissolving evaporite rocks when they come into contact with them. Both underground quarries and a succession of boreholes that have intercepted the basal limestone bed at the beginning of the evaporite sequence have yielded water that is a mixture of the two previously discussed waters ("mixed water"—MW samples in Fig. 19) [49].

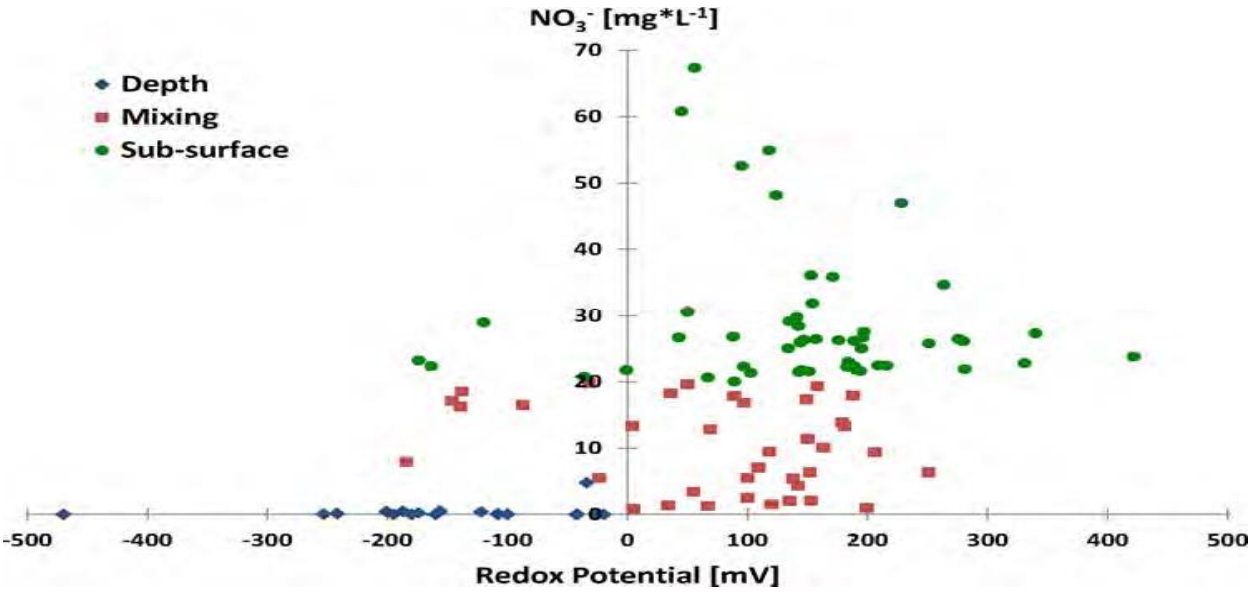

Figure 19 shows the chemical composition of the three types of water in the Moncalvo cave region.(Hypogene Gypsum Caves in Piedmont (N-Italy) Chapter · August 2017) [50].

3) Theory of Spelegenesis

The cave is unquestionably of the phreatic variety and was created in a region where speleogenesis took advantage of all the evaporite rock fissures. The cave is perfectly level along a horizontal plane that appears to be linked to the former elevation of the local water table, despite the fact that the gypsum beds dip by 10°. There are two potential sources for the replenishment of this aquifer: surface infiltration water and deeper circulating water. The River Tanaro, which runs about 30 meters below the cave floor, is nearby and close by. This river may have intercepted the gypsum bed during the entrenchment of the fluvial network, resulting in a local base level and karstification period. We think that this tunnel is an excellent illustration of intrastratal karst, where waters rising from below have carved the maze system out of every possible discontinuity. In reality, the lower aquifer-feeding evaporite rocks in this region's Messinian stratigraphic sequence are surrounded by thin beds of relatively permeable sediments (sands). Given the higher dissolution in the lower section of the cave passages relative to the ceiling, the conduit morphologies plainly show that some of the waters originated below. Since there are no alluvial sediments, it appears that floodwater did not create the maze design. Unfortunately, the substantial sediment deposits totally obscure the original floor, concealing any feeder tunnels [51].

Figure 20 Moncalvo shows a tiny, nearly vertical conduit on the cave floor.(Hypogene Gypsum Caves in Piedmont (N-Italy) Chapter · August 2017).

Figure 21 Monticello d'Alba: detail of the intercepted tunnel labyrinth and the gypsum quarry.(Hypogene Gypsum Caves in Piedmont (N-Italy) Chapter · August 2017) [52].

Figure 22 The triangular cross section of Monticello d'Alba with the wider portion downward.(Hypogene Gypsum Caves in Piedmont (N-Italy) Chapter · August 2017).

2.2 MURISENGO QUARRY

1) The Chaotic compound known as Valle Versa is the Murisengo Quarry.

This Stop is situated in the VVC and is near the Villadeati fault in a subterranean quarry. Layers of clastic gypsum (gypsrudites and gypsarenites) and a fine-grained matrix are exposed along with gypsum blocks varying in size from a few meters to several tens of meters. The latter consists of clay chips and marly clasts that range in size from mm to m, some of which are derived from the lower Messinian Sant'Agata Fossili marls. Cyclic successions of the PLG unit are maintained in the biggest blocks. We will pay close attention to a block made up of four rounds in particular. The single gypsum strata are up to ten meters thick and made of massive selenite that transition to banded selenite as it rises. It is possible to see stunning formation cones at the base of these layers [53].

2) The Mine at Verrua Savoia

The Verrua Savoia quarry reveals a VVC-attributed chaotic sequence (Clari et al., 2004). Pliocene sediments from the Argille Azzurre Fm are deposited on top of this erratic succession (Figs. 23, 24). Now safeguarded as a geosite, this quarry has informational panels (Zunino et al., 2012). Soft mud breccia's with sheared textures were seen intruding the chaotic complex during quarry action (Figs. 23, 24). Unfortunately, due to the alteration of the quarry front and significant weathering of the outcrop, these relationships cannot be seen today. On the quarry front, however, more durable volumes of carbonate-cemented rocks that were formerly contained within the soft breccia's are still discernible, both in situ and accumulating (Figs. 23, 24). By utilizing authigenic dolomite, it is possible to distinguish between two primary types of rocks: 1) strongly lithified matrix-supported breccias with sharp or diffuse borders to the host unlithified breccias, ranging in size from dm to m. (Fig. 24). The planktonic foraminifer-rich marly wackestone that makes up the clasts was mined from the underlying Miocene sequence.The encasing soft mud breccias' structure and composition are comparable in the cemented masses, but the degree of lithification varies [54].

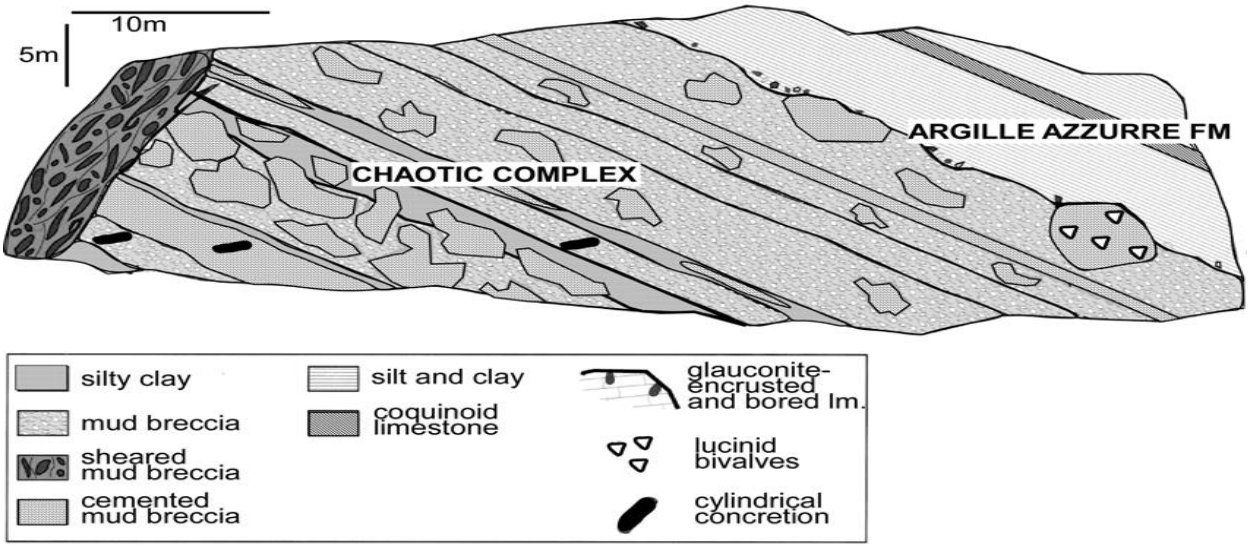

Figure 23 shows a cross-sectional diagram of the top portion of the VVC as it was discovered in the Verrua Savoia quarry in (2004) Clari et al. (The northernmost record of the Messinian salinity crisis (Piedmont basin, Italy Article in Geological Field Trips · November 2016)

The chemosymbiotic taxon Lucina sp. has clusters of articulated and disarticulated bivalve shells (Fig. 23). 2) Circular concretions with a diameter of about 10 cm and a length of more than 1 m composed of light-colored marly limestones (Fig. 23). They exhibit rounded, smoothed edges and crosscut the bedding surfaces at steep angles. The concretions' axial portion could either be completely empty or, more frequently, contain sediments (Fig. 23) [55].

Figure 24 A panoramic picture of the Verrua Savoia quarry showing large, recognizable cemented masses. B) High-angle, cross-cutting cylindrical concretions (shown by arrows) in the bearing planes. C) Polished block of cylindrical concretion with dark sediment filled axial section. D) A cement brick in detail. Recognizable molds belong to the chemosymbiotic bivalve Lucina sp (arrows). E) Mud breccias with an obvious sheared structure. (The northernmost record of the Messinian salinity crisis (Piedmont basin, Italy Article in Geological Field Trips · November 2016)[56].

Dolomite makes up the majority of the intergranular cement in both types of rocks, and it exhibits low 13C values (from -23 to -10 PDB) and high 18O values up to +7 PDB. The markedly positive 18O signature, which is present in all of the cylindrical concretions, may be proof of the destabilization of gas hydrates, while the 13C values demonstrate carbonate precipitation brought on by microbial oxidation of methane (Clari et al., 2004; 2009).

A lag of silty clay clasts stained with glauconite marks the upper boundary between the chaotic sequence and the subordinate Pliocene layers. This boundary is marked by a sharp erosional surface. Because of the boulder-sized bodies of Lucina-bearing breccias described above, this surface becomes extremely irregular in some areas (Fig. 23). These masses' lateral and top surfaces are bored. Recognizable are centimeter-long Trypanites-like borings that are packed with phosphatized and glauconitized sediments. The same surfaces also contain tiny crusts of glauconite.

On the basis of a comparison with contemporary instances, Clari et al. (2004) have concluded that the chaotic succession exposed at Verrua Savoia represents the geological record of a Messinian mud volcano. greasy mud and Unconsolidated mud breccias were erupted from the mud volcano crater and flowed along its sides during brief paroxistic periods, as evidenced by semilithified clasts sourced by the underlying sedimentary succession (Fig. 24) [57].

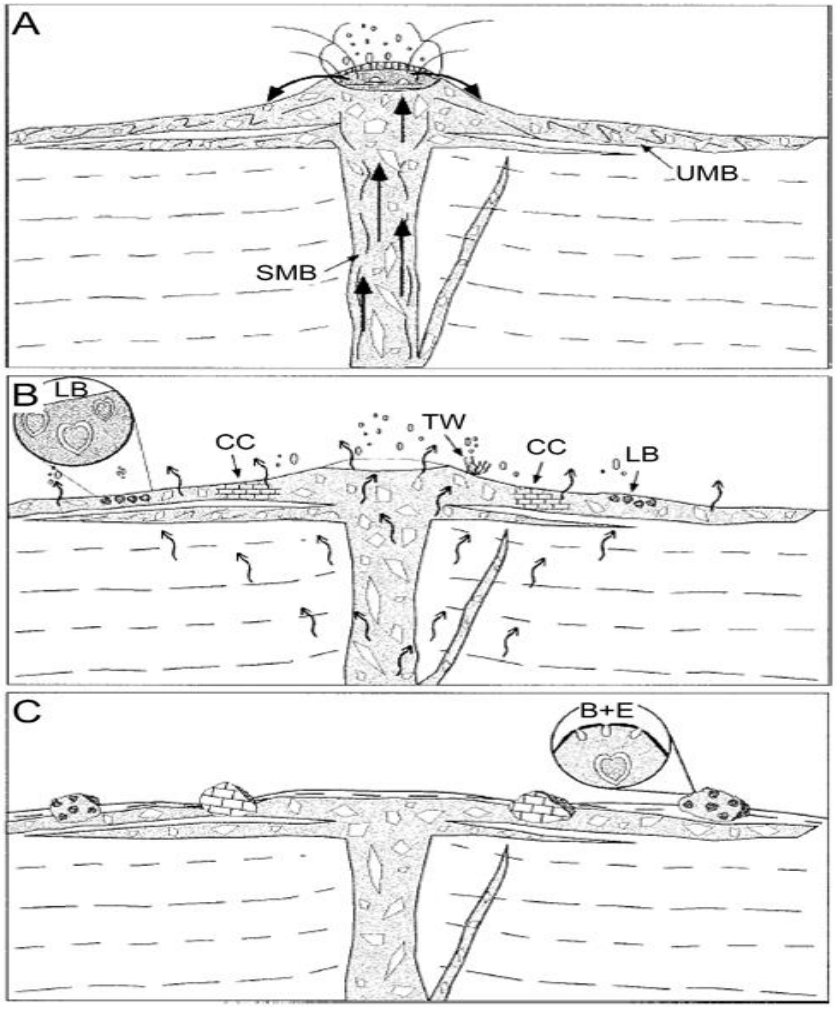

Figure 25 is a schematic drawing illustrating the various stages of the submerged mud volcano's activity (from Clari et al., 2004). A) During brief bursts of paroxysmal activity, a mud volcano's explosion creates an irregular cone-shaped structure made of unsheared mud breccias (UMB). In the duct, sheared mud breccias (SMB) are created. B) Slow and widespread degassing is a hallmark of prolonged quiescence. Chemosymbiotic taxa congregate and reside close to the seeps in colonies. In this stage, methane is regionally degraded by microbes in a process known as carbonate precipitation (CC, carbonate cementation; TW, tube worms; LB, lucinid bivalves). C) The cone-shaped building is partially destroyed after a clay volcano extinguishes (B+E: boring and encrustations). (The northernmost record of the Messinian salinity crisis (Piedmont basin, Italy Article in Geological Field Trips · November 2016).

Due to the ongoing, slow-rate expulsion of methane-rich fluids throughout the entire mud volcanic edifice, localized cementation of the mud breccias and their colonization by chemosymbiotic bivalves occurred over extended periods of quiescence (Fig. 24). Due to the localized cementation of specific portions of the mud volcano edifice's flanks, the cylindrical concretions actually represent the mud volcano's plumbing system (for a contemporary analogous, see Diaz del Rio et al., 2003). The cemented masses were exhumed and exposed at the sea bottom at the end of mud volcano activity, just before the deposition of Pliocene marine sediments, according to drilling and glauconite crusts on the exterior of the masses (Fig. 24).

3) Data from the micropaleontology of the Pliocene Strata

About 80 meters of well-stratified marly clays, silts, and sandy silts, affected by faults, with interbedded sand and calcarenite banks, increasingly more frequent and thicker upwards, make up the Pliocene succession (Dela Pierre et al., 2003; Violanti, 2012). In the upper transect, only sandy silts, sands, and calcarenites are found. Foraminiferal preservation was usually subpar; samples were covered in calcareous aggregates or only partially included. Reworked tests are prevalent and include Miocene to lower Pliocene taxa in the middle and higher layers, as well as Eocene forms in the lower section. Miocene to Pliocene taxa like Globoturborotalita decoraperta, Globigerinoides obliquus, Globigerinoides extremus, and less frequently N. acostaensis are the primary contributors to planktonic foraminiferal assemblages. On the basis of the co-occurrence of Globorotalia margaritae and Globorotalia puncticulata, the lower portion of the marly clays and silts were correlated to the MPl3 Zone; the subsequent sandy silts and calcarenites, which produced G. puncticulata and G. puncticulata padana, were correlated to the MPl4a Zone. Anomalinoides helicinus, Cassidulina carinata, Cibicidoides pseudoungerianus, Hoeglundina elegans, Planulina ariminensis, Siphonina reticulata, Uvigerina peregrina, and U. rutila are among the prevalent deep outer neritic to bathyal taxa found in the reasonably in situ (not reworked) benthic for (Van Morkhoven et al., 1986). There aren't many of the infaunal, stress-tolerant Bolivina, Brizalina, and Bulimina species, which favor muddy sediments. Inner neritic taxa (Elphidium spp., Neoconorbina terquemi, and Cibicides spp.) are prevalent in the uppermost sands and calcarenites, indicating that the basin is shallowing [58].

4) Production and Shift

The cultivation must satisfy an annual production requirement of 150,000t. To optimize operations and reduce downtime guaranteeing greater continuity of material flow in the crusher, two attachments are kept active at the same time. The operations in the two sites are staggered so that while drilling is being carried out in one, the mucking is carried out in the other.

The operations are carried out on a daily shift of 08 hrs.

- Drilling 03 hrs
- Loading 1.5 hrs

- Muck 3-4 hrs

The cleaning is done using a loader shovel and trucks (approx.10 m3) which go up to helical ramp to go and unload at the crusher. The scaling operations are carried out by means of ripper tooth mounted on the excavator arm. The product characteristics of the size leaving the crusher are 0-40mm [59].

5) Monitors

The monitoring carried out is essentially of two types: tension and deformation. The stress analysis is performed through the use of flat jacks inserted inside some pillars of fourth level. These measurements are constantly compared with the results provided by a numerical model and confirm that the stresses inside a pillar are not constant but in the central part they are more modest than at the edges. The deformation analysis is essentially a convergence of the tunnels at the pillars [60].

CHAPTER 03

3.1 MATERIALS AND METHODS

1) SAMPLING, TESTING AND DATA PROCESSING

SPECIMEN DESCRIPTION

From the visit of Monclavo Mining site, we obtained the samples of Gypsum, from which we have obtained following 06 samples: 03 fine grained specimens and 03 coarse grained specimens.

Figure 26 Moncalvo Mine visit 2023.

Figure 27 Monclavo Mine Visit 2023.

Figure 28 Moncalvo Mine visit 2023.

Figure 29 Moncalvo Mine visit 2023.

FINE GRAINED SPECIMEN:

Fine grained gypsum can be defined as in which the individual grains or crystals with in the material are very small and closely packed together resulting in a smooth or uniform appearance when viewed under a microscope or with the naked eye.

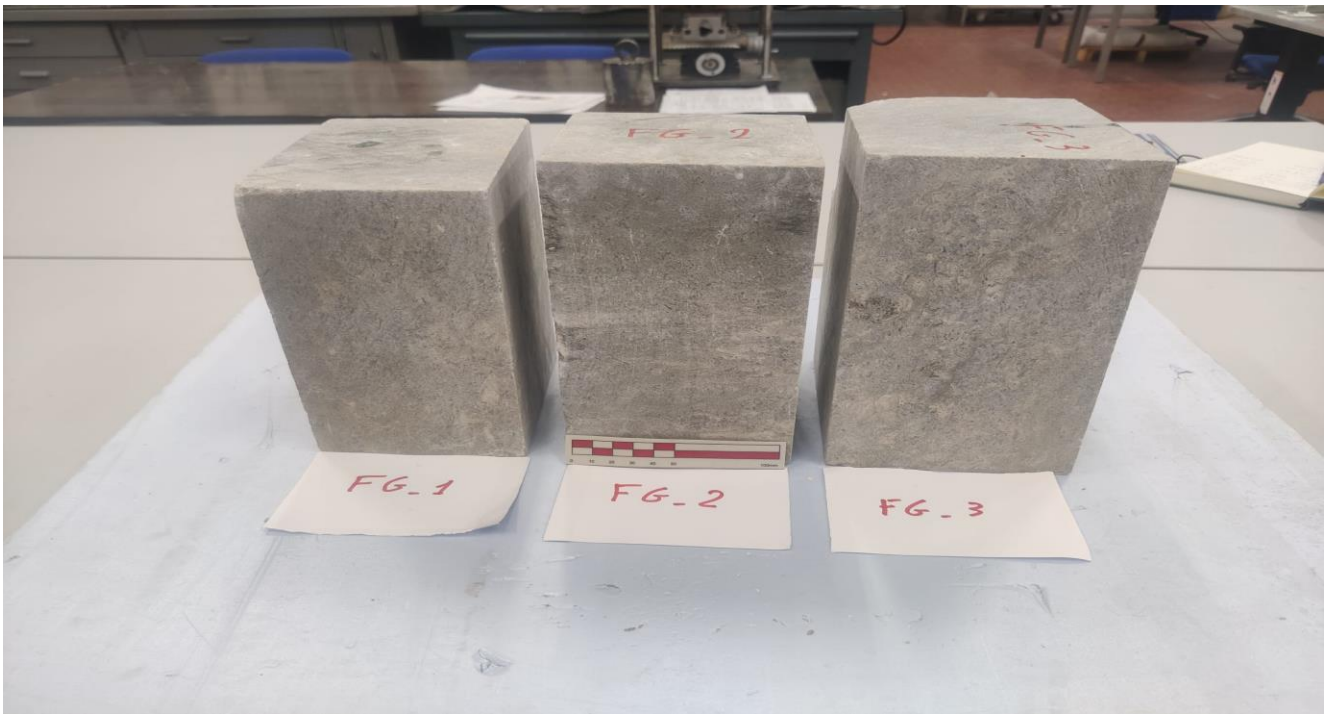

Figure 30 shows the fine grained specimens of gypsum obtained from the samples, on which testing have been performed.

Following are the Base surface Area, Volume and Unit weight of each specimen.

FINE GRAINED 01

Base Surface Area: 13332 mm square
Volume: 2546412 mm cube
Unit weight= weight of specimen/ volume of specimen
5571g/2546412mmcube= 2.187 E -3 g/mm cube

FINE GRAINED 02

Base Surface Area: 10807 mm square
Volume: 2183014 mm cube
Unit Weight= weight of specimen/ volume of specimen
4861g/2183014 mm cube= 2.226 E-3 g/mm cube

FINE GRAINED 03

Base Surface Area: 14472 mm square
Volume: 2995704 mm cube
Unit Weight = weight of specimen/ volume of specimen
6652g/2995704 mm cube = 2.22 E-3 g/mm cube

COARSE GRAINED 01

Base Surface Area: 14124 mm square
Volume: 2683560 mm cube
Unit weight= weight of specimen/ volume of specimen
5884g/2683560 mm cube = 2.193 E-3 g/ mm cube

COARSE GRAINED 02

Base Surface Area: 15840 mm square
Volume: 3025440 mm cube

Unit weight= weight of specimen/ volume of specimen
6982g/3025440 mm cube = 2.308 E-3 g/mm cube

COARSE GRAINED 03

Base Surface Area: 12792 mm square
Volume: 2276976 mm cube
Unit weight= weight of specimen/ volume of specimen
5129g/2276976 mm cube =2.252 E-3 g/ mm cube

The Catman Easy by HBM acquisition system was utilized, testing was conducted on Galdabani testing equipment, and load was detected using a load cell HBM of 100 tons of full scale. Two LDVT transducers (HBM, range 50mm, precision 0.01mm) have been used to measure specimen settlement.

WORKING OF FINE GRAINED SPECIMEN 01

We are calculating now the stress and strain of fine grained specimen 01.
Before Testing:

Figure 32 shows the testing procedures performed on sample fine grained specimen 01

From the stresses and strains we have obtained the following results.

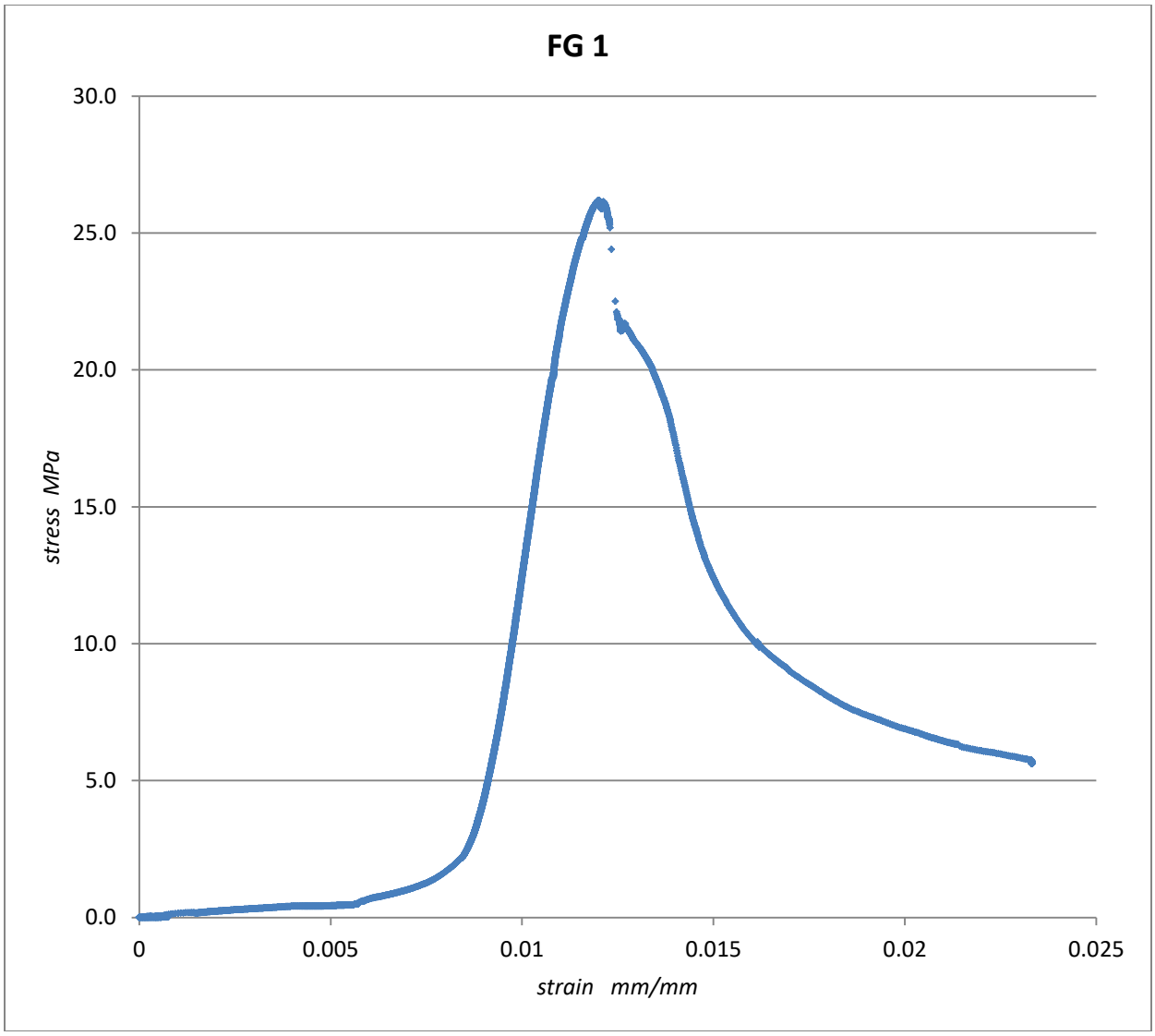

Figure 33 shows the stress and strains evaluation of the specimen.
After Testing:

Figure 34 shows the failure of specimen after testing

From the test we have obtained the following results
Uniaxial Compressive Strength= 25.75MPa
Pundit time us@250kHz/54kHz= 50
Pundit velocity m/s= 3820m/s
Dynamic Modulus= 3.19 E 10 MPa
Static Modulus= 1840 MPa

WORKING OF FINE GRAINED SPECIMEN 02
We are calculating now the stress and strain of fine grained specimen 02.
Before Testing:

Figure 35 shows the testing procedures performed on sample fine grained specimen 02

From the stresses and strains we have obtained the following results.

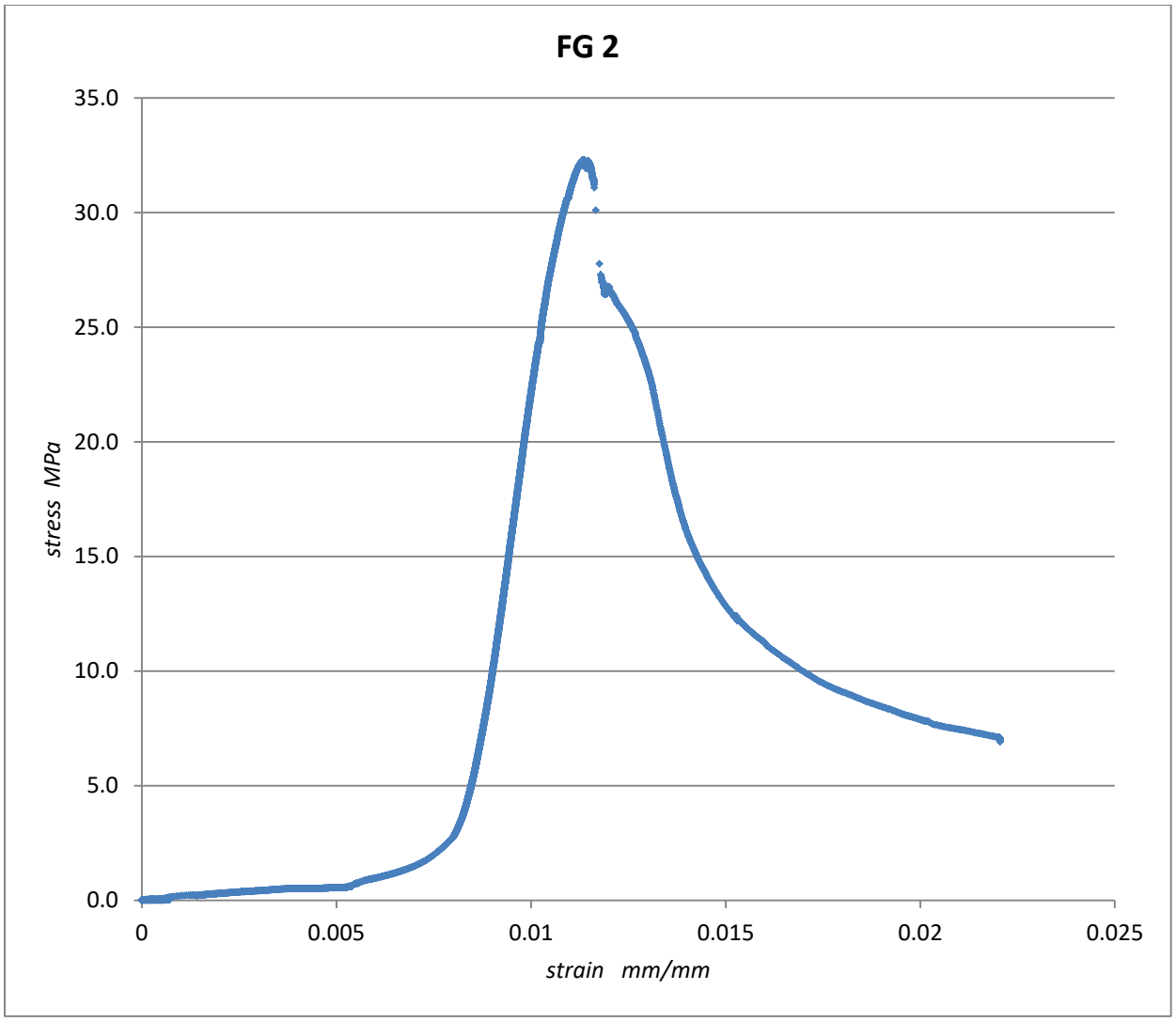

Figure 36 shows the stress and strains evaluation of the specimen.

After testing:

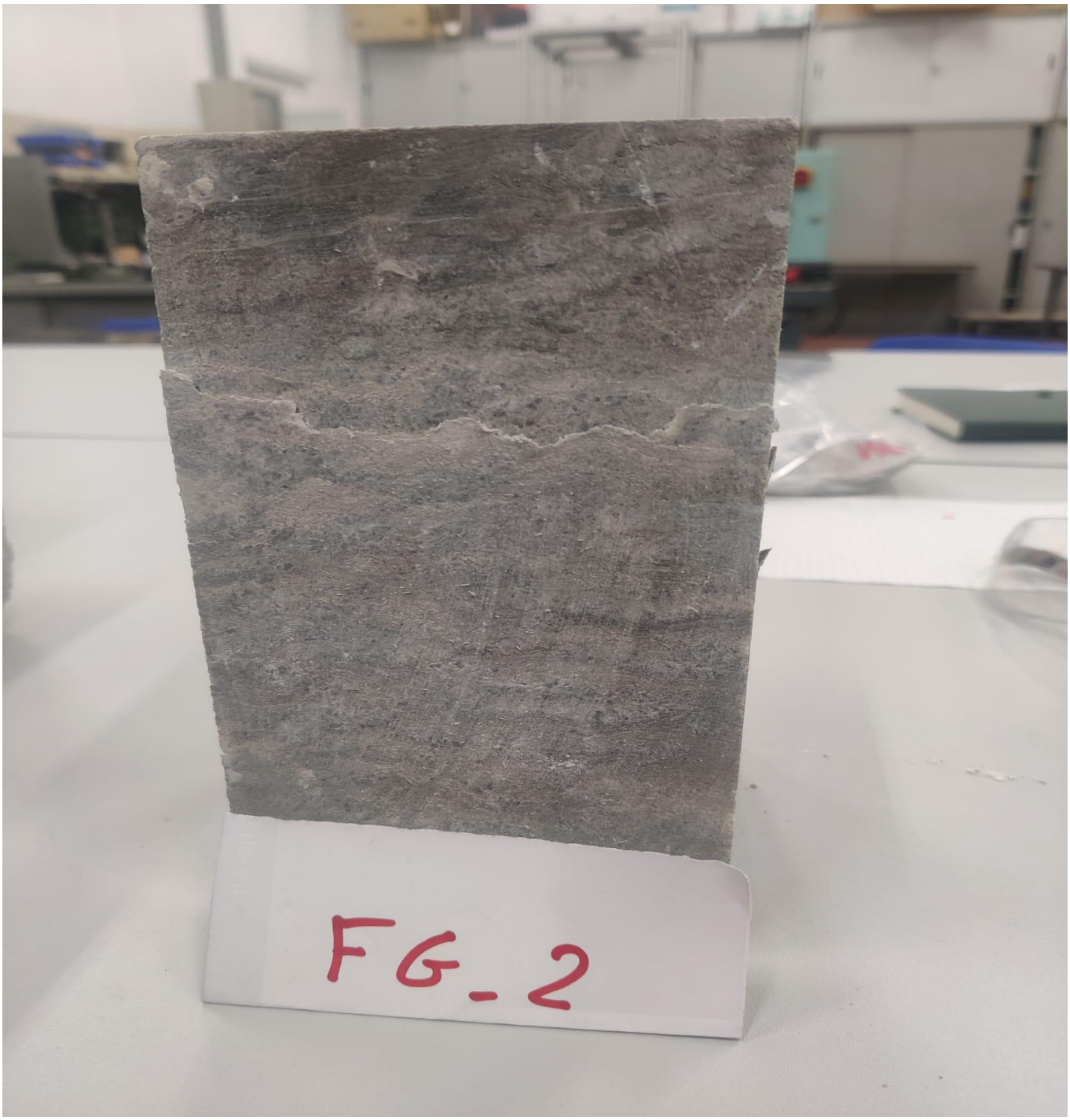

Figure 37 shows the failure of specimen after testing

From the test we have obtained the following results
Uniaxial Compressive Strength= 30.70MPa
Pundit time us@250kHz/54kHz= 50
Pundit velocity m/s= 4040m/s
Dynamic Modulus= 3.63 E 10 MPa
Static Modulus= 2420 MPa

WORKING OF FINE GRAINED SPECIMEN 03

We are calculating now the stress and strain of fine grained specimen 03.
Before Testing:

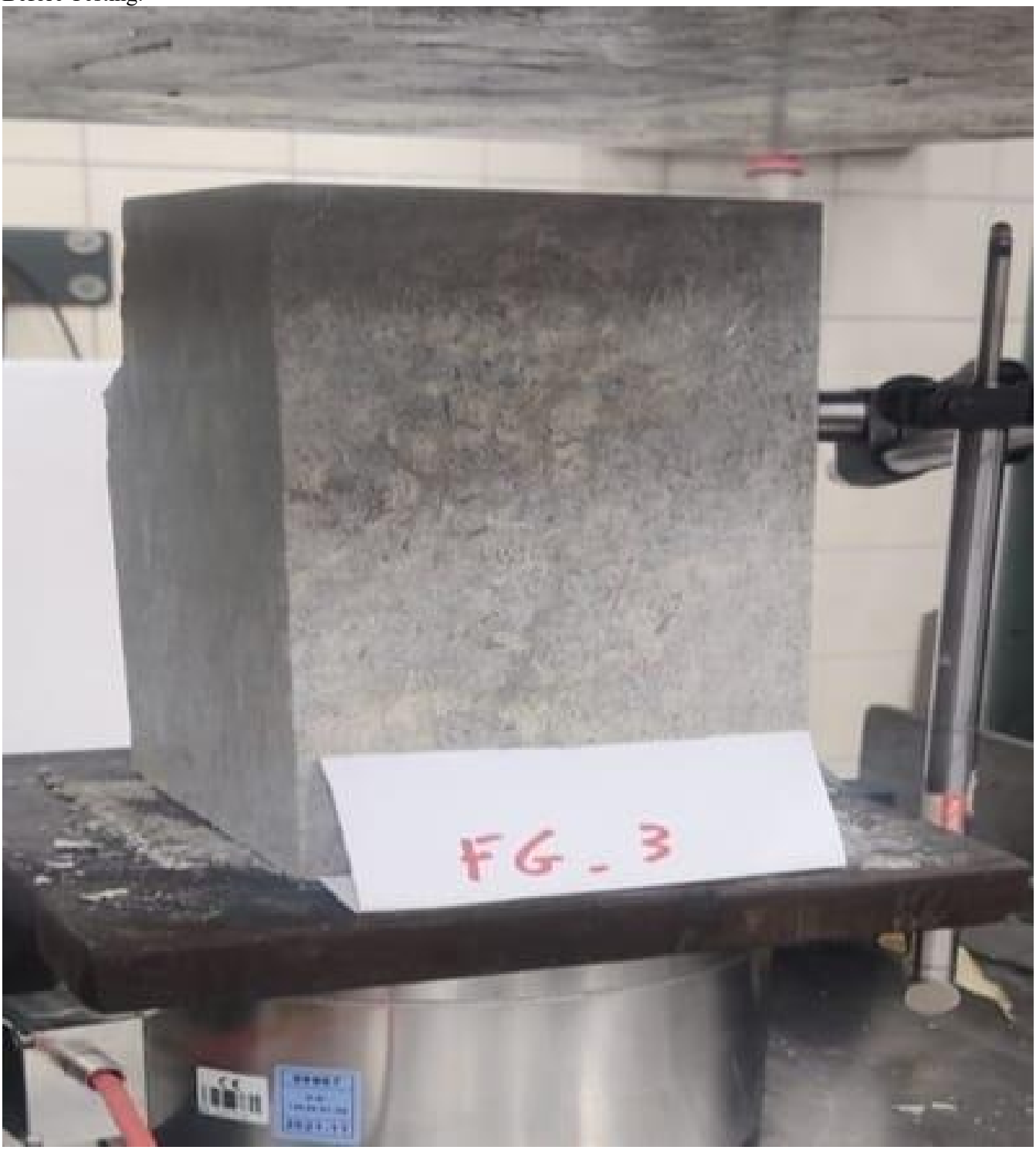

Figure 38 shows the testing procedures performed on sample fine grained specimen 03
From the stresses and strains we have obtained the following results.

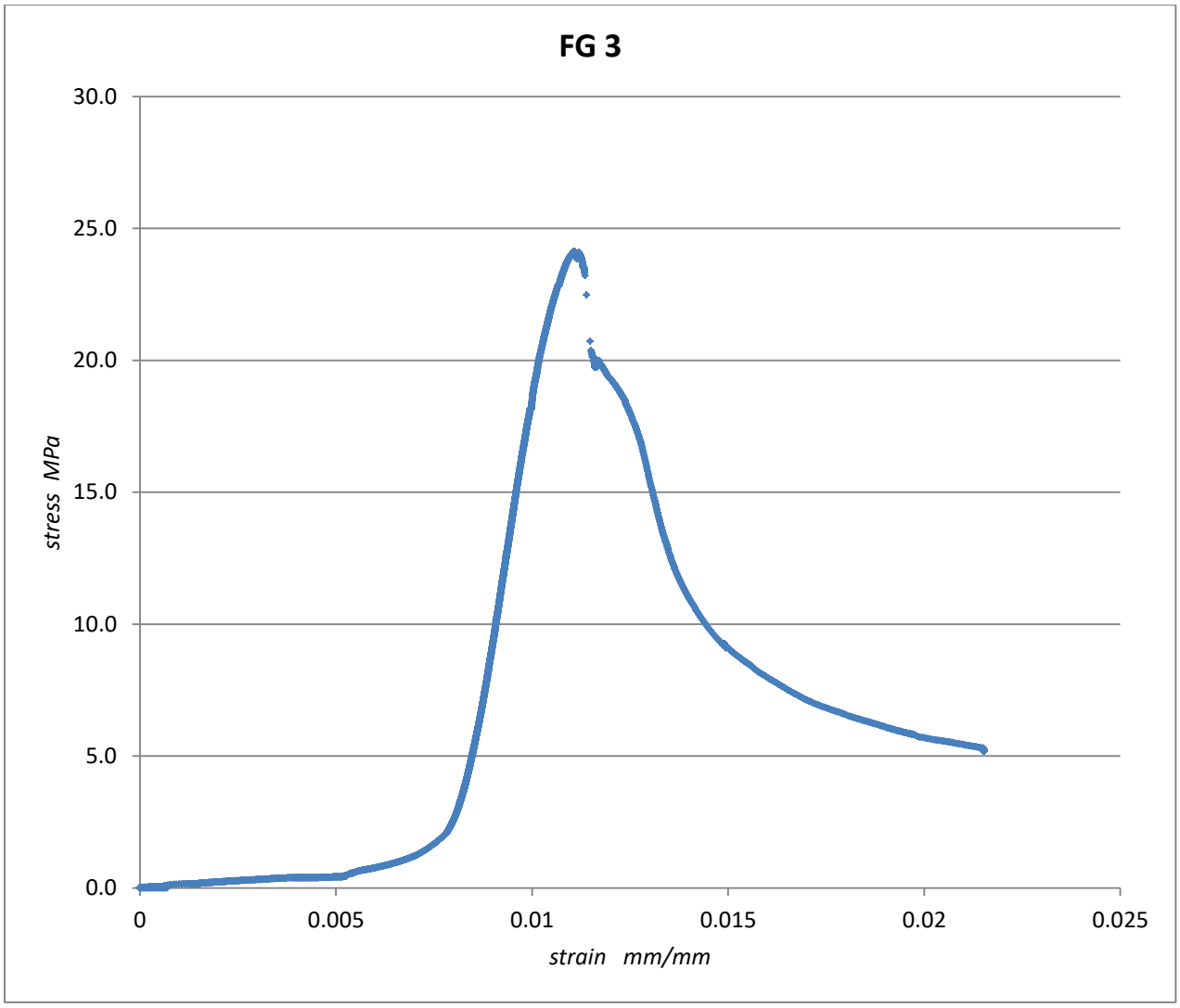

Figure 39 shows the stress and strains evaluation of the specimen.

After testing:

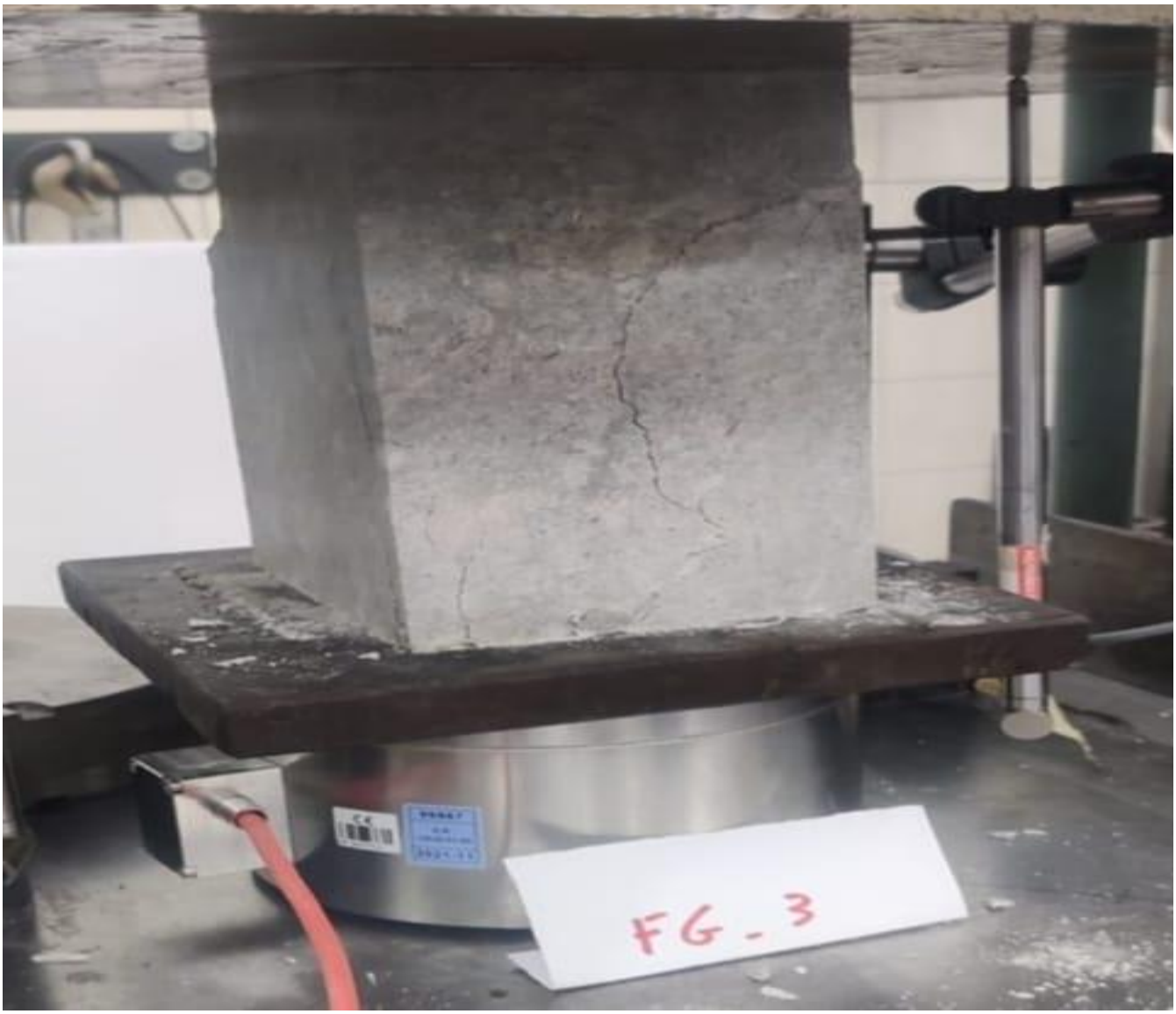

Figure 40 shows the failure of specimen after testing

From the test we have obtained the following results
Uniaxial Compressive Strength= 23.50MPa
Pundit time us@250kHz/54kHz= 46
Pundit velocity m/s= 4500m/s
Dynamic Modulus= 4.49 E 10 MPa
Static Modulus= 1880 MPa

WORKING OF COARSE GRAINED SPECIMEN 01
We are calculating now the stress and strain of fine grained specimen 01.
Before Testing:

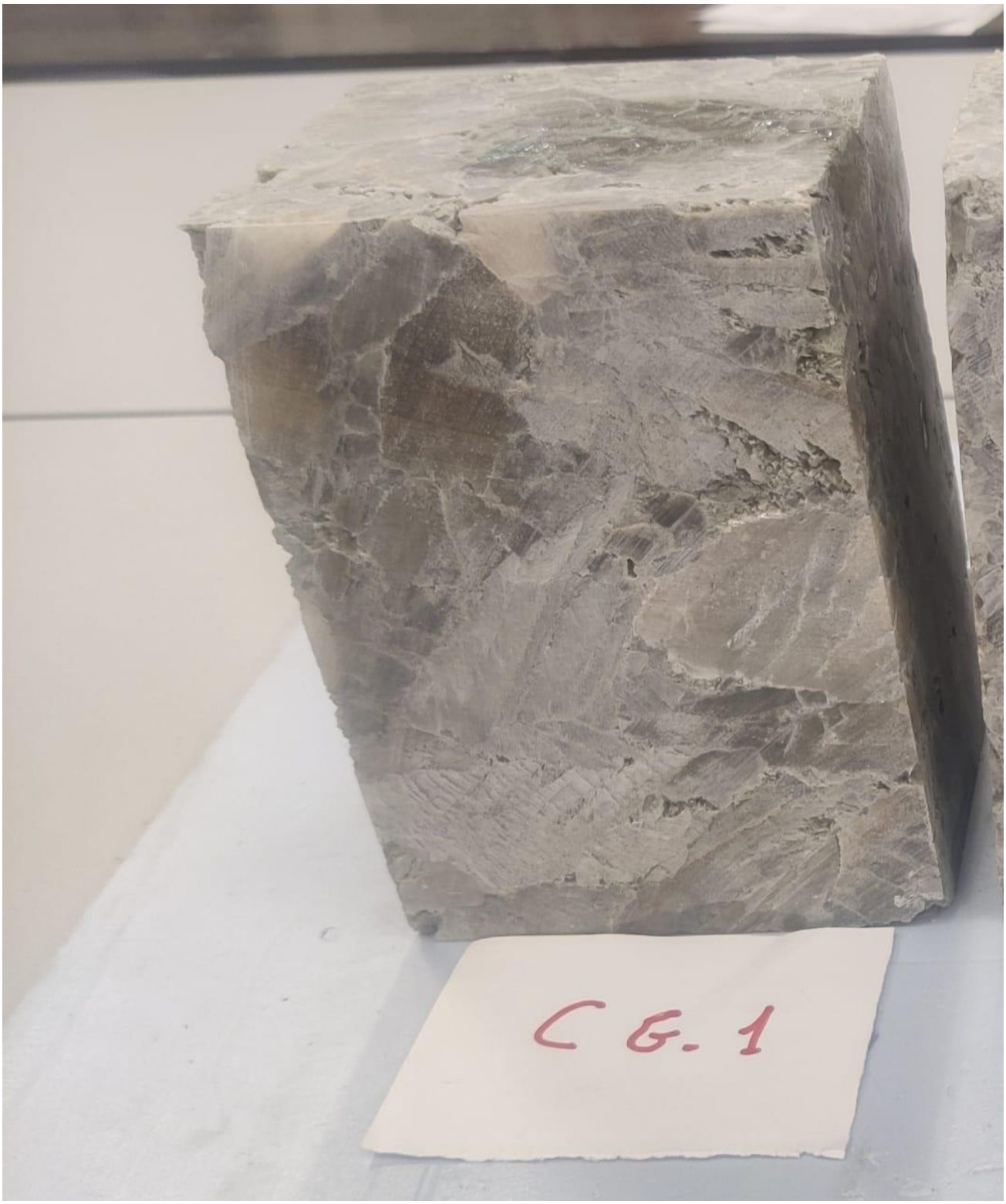

Figure 41 shows the testing procedures performed on sample coarse grained specimen 01

From the stresses and strains we have obtained the following results.

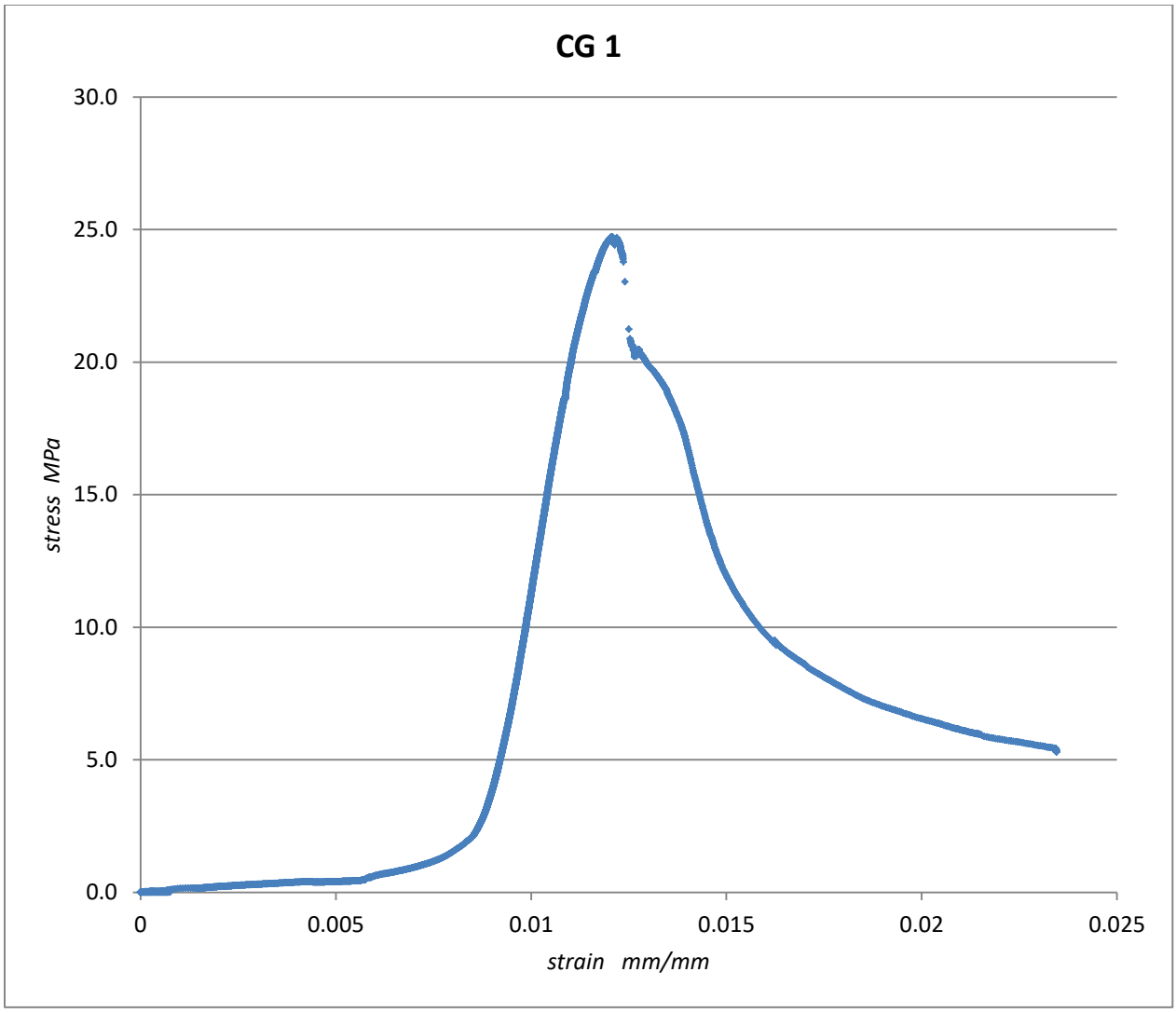

Figure 42 shows the stress and strains evaluation of the specimen.

After testing:

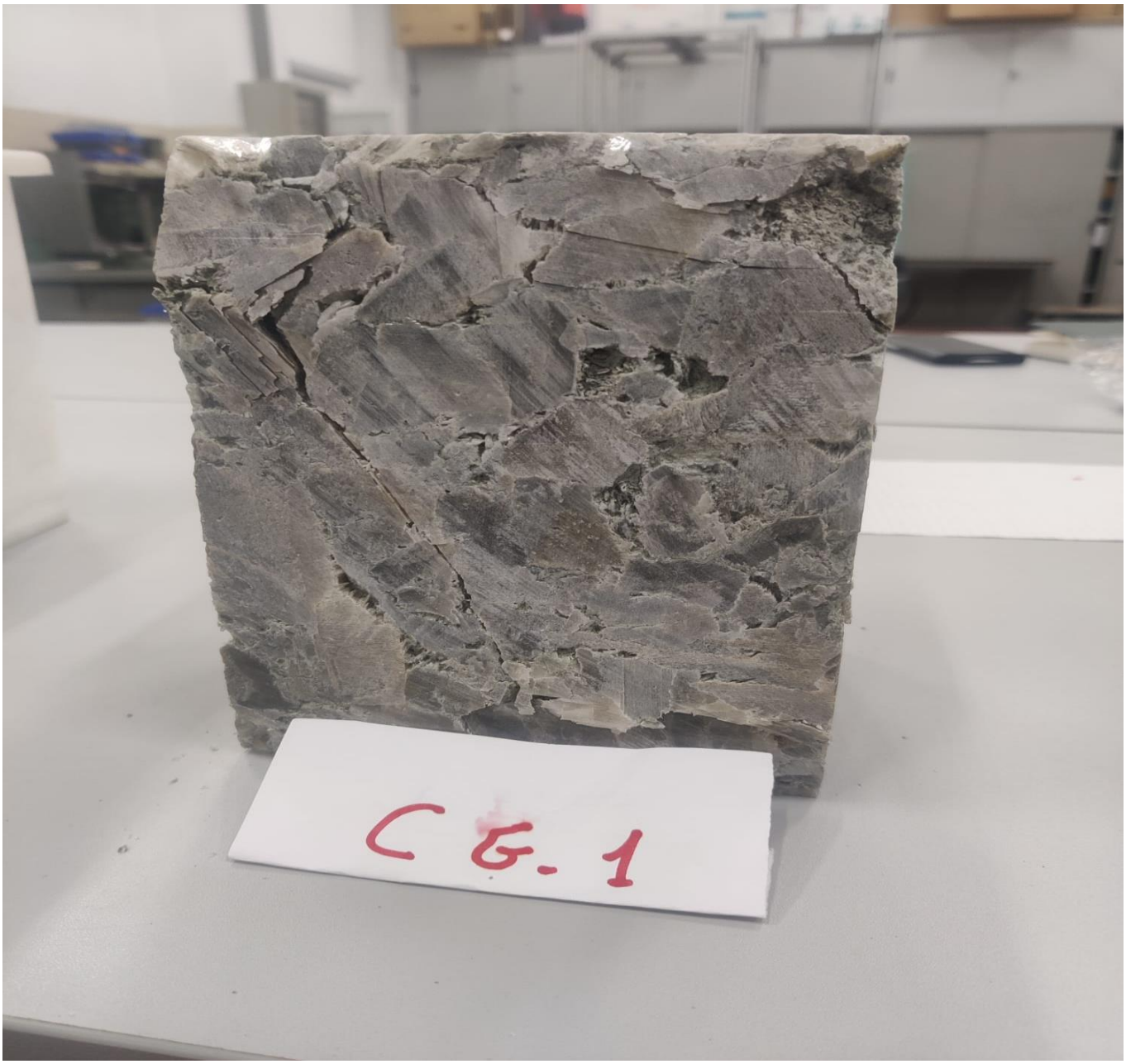

Figure 43 shows the failure of specimen after testing

From the test we have obtained the following results
Uniaxial Compressive Strength= 24.40MPa
Pundit time us@250kHz/54kHz= 65-50
Pundit velocity m/s= 2923/3800m/s
Dynamic Modulus= 1.87 e10/3.16 e10 MPa
Static Modulus= 1740 MPa

WORKING OF COARSE GRAINED SPECIMEN 02
We are calculating now the stress and strain of coarse grained specimen 02.
Before Testing:

Figure 44 shows the testing procedures performed on sample coarse grained specimen 02

From the stresses and strains we have obtained the following results.

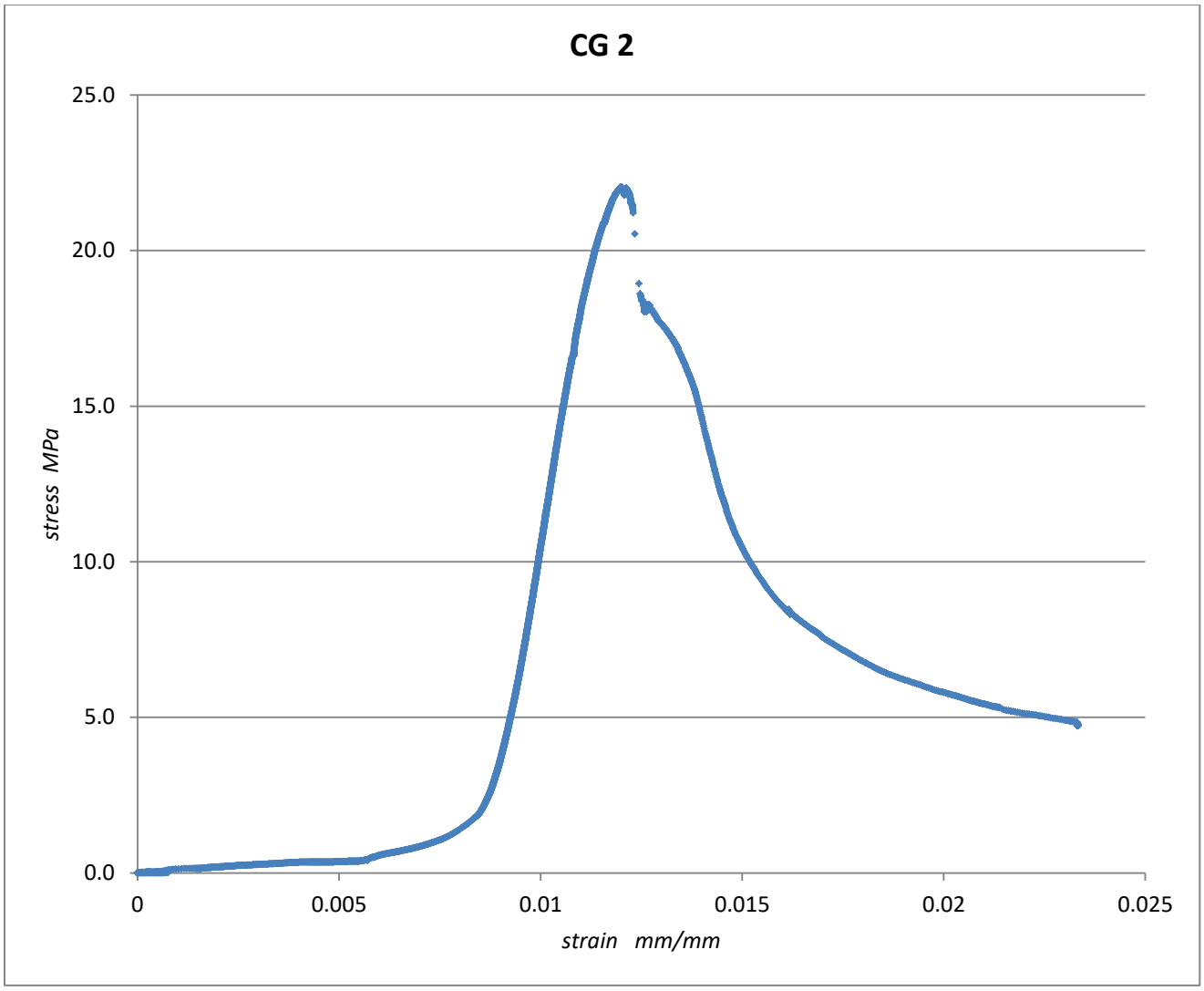

Figure 45 shows the stress and strains evaluation of the specimen.

After testing:

Figure 46 shows the failure of specimen after testing

From the test we have obtained the following results
Uniaxial Compressive Strength= 21.63MPa
Pundit time us@250kHz/54kHz= 52
Pundit velocity m/s= 3654/4050m/s
Dynamic Modulus= 3.08 e10/3.78 e10MPa
Static Modulus= 1560 MPa

WORKING OF COARSE GRAINED SPECIMEN 03
We are calculating now the stress and strain of coarse grained specimen 03.
Before Testing:

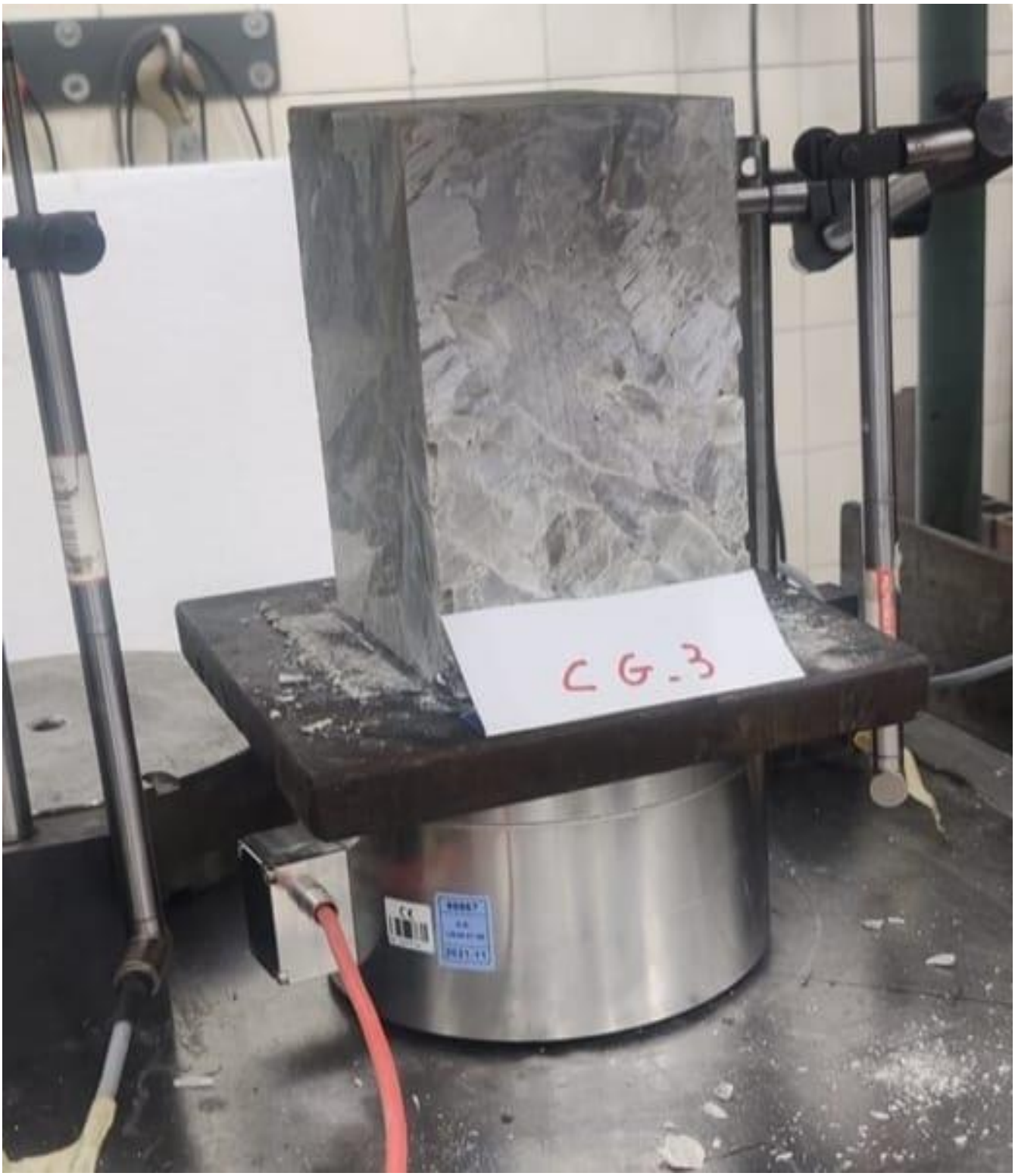

Figure 47 shows the testing procedures performed on sample coarse grained specimen 03

From the stresses and strains we have obtained the following results.

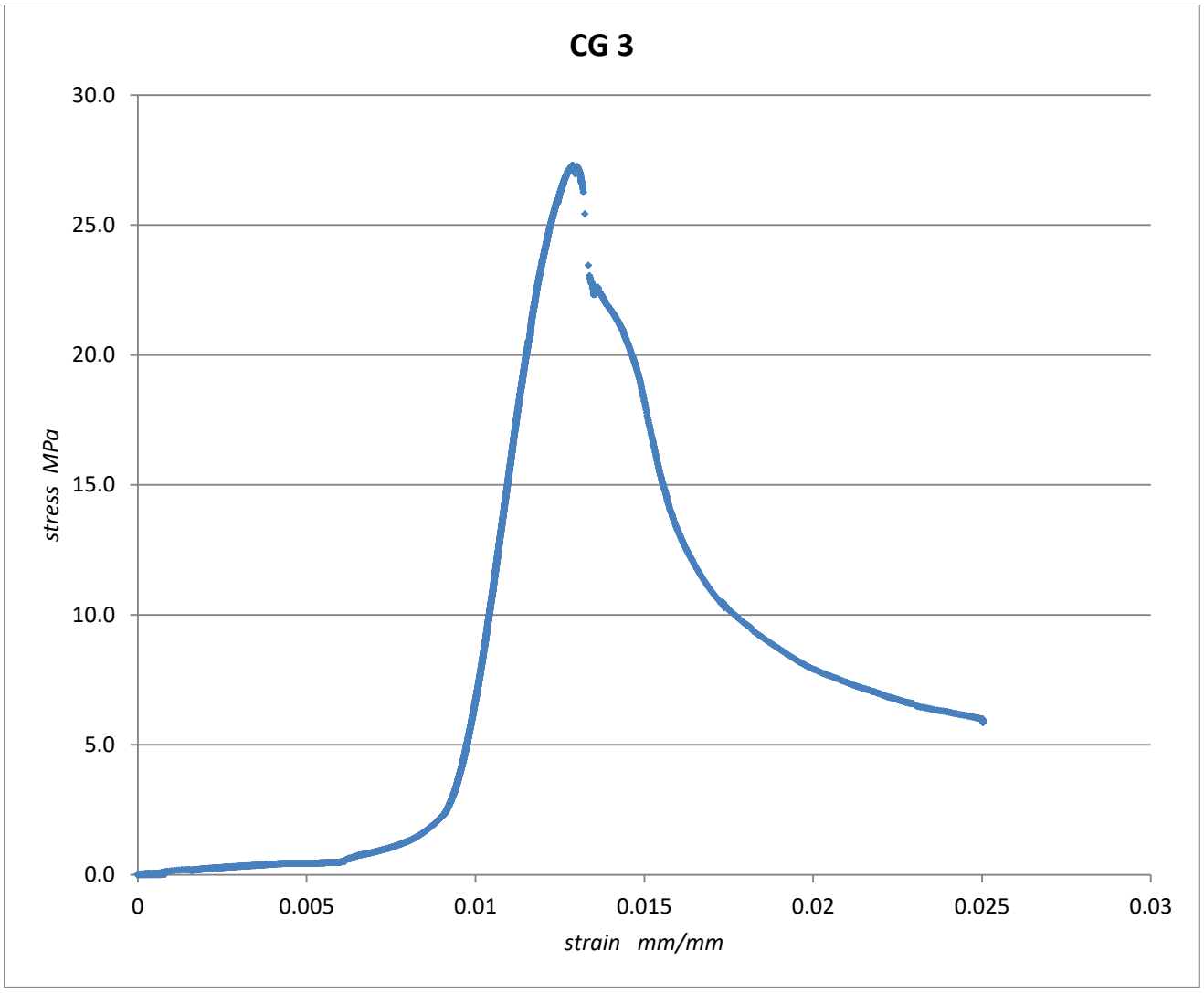

Figure 48 shows the stress and strains evaluation of the specimen.

After testing:

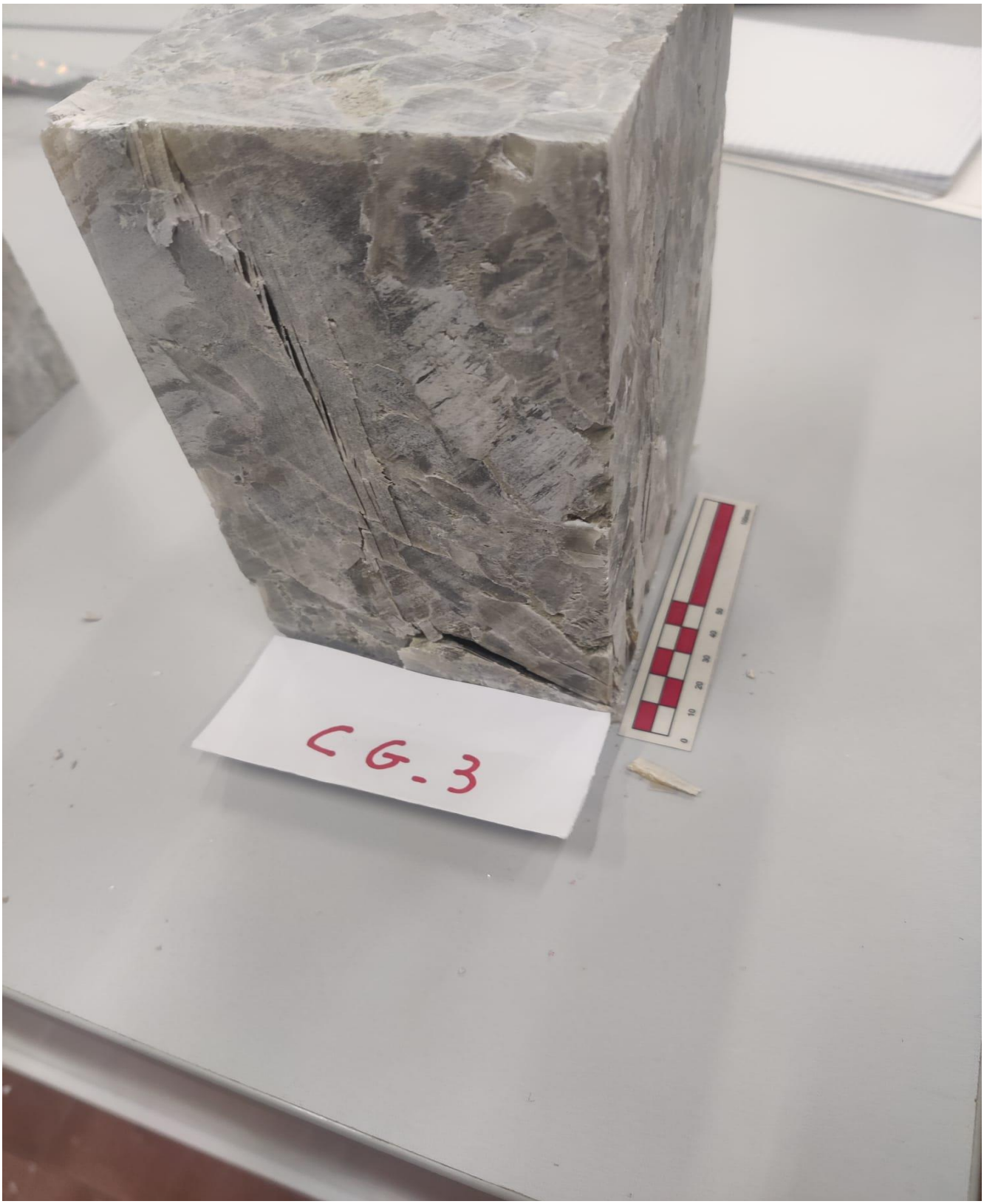

Figure 49 shows the failure of specimen after testing

Figure 50 shows the failure of specimen after testing

From the test we have obtained the following results
Uniaxial Compressive Strength= 24.40MPa
Pundit time us@250kHz/54kHz= 65-50

Pundit velocity m/s= 3654/4050m/s
Dynamic Modulus= 3.08 e10/3.78 e10MPa
Static Modulus= 1840 MPa

From a crystallographic perspective, gypsum exhibits a layered structure, characterized by the arrangement of calcium ions and sulfate tetrahedral forming adjacent pairs of sheets. These sheets are separated by double layers of water molecules, which contribute to the distinct cleavage observed in gypsum crystals.

The crystal-scale anisotropy of gypsum plays a significant role in governing its fundamental physical characteristics, including mineral rheology, as initially proposed by Craker and Schiller (1962). In their research, the authors conducted experiments on the deformation of individual gypsum crystals using a three-point loading system. They demonstrated that when stress is applied perpendicular to the mineral cleavage plane (010 plane), the crystal undergoes bending and shows notable plastic deformation, even at relatively high strain rates. Conversely, when stress is applied parallel to the cleavage plane, the crystal fracture before any noticeable bending occurs.

At the scale of rock formations, the diversity of gypsum facies worldwide leads to a wide spectrum of mechanical strength values, both in uniaxial and triaxial loading scenarios. This variability encompasses differences in grain size, porosity, gypsum content, and rock structure (Papadopoulos et al., 1994; Yilmaz, 2007; Caselle et al., 2019a, Caselle et al., 2019b). Under triaxial loading, gypsum can display micro-plasticity due to grain kinking (Brantut et al., 2011, Caselle et al., 2020a, Caselle et al., 2020b).

Our experimental investigation aims to quantify the stresses and strains, and Modulus of Elasticity of all the specimens. We conducted investigations involving uniaxial compression tests, uniaxial creep tests, and conventional triaxial experiments. Microstructural analysis was carried out on deformed samples to elucidate the mechanisms underlying gypsum deformation and failure.

On average, specimens with finer grains are stronger than those with coarser grains. Every specimen exhibits a peak strength followed by a corresponding decrease in residual strength, as seen by the specimens' prolonged deformation following failure [68].

We begin the specimen preparation process with blocks, and we prepared them by seeding the prismatic element's surface. Being cautious to prevent harm to all of the materials. This established the attainment of highly significant strength levels. The linear elastic portion is the last point to be considered because it provides evidence. Since all of the variables come from the graph, we can compute stress or strain both graphically and numerically. We assume that stress or strain equals the modulus of elasticity. Strength is determined by both the grain size distribution and statistical statistics, which are at least twice as large.

CHAPTER 04

4.1 ANALYSIS AND DISCUSSION

In the Monferrato region, the depth of the evaporite layers shows significant variation (from 0 to 140 meters), a result of considerable erosion that occurred at the conclusion of the evaporite cycle, affecting the gypsum layers. It is likely that epigenic quarries were formed during this brief period of exposure in the intra-Messinian era. Sediments found within these quarries, comprising both benthic and planktonic foraminiferal groups, span from the Burdigalian to the Upper Pliocene epochs. These deposits are thought to have been laid down relatively recently, although it's not entirely dismissible that they could have been placed in caves that formed in the late Messinian period. The genesis of the area's most significant quarries likely began towards the end of the Messinian period under epigenic conditions. Over time, particularly throughout the Quaternary period, these pre-existing quarries may have gradually expanded within a hypogene karst system that was both intrastratal and confined. (To cite this article: Bartolomeo Vigna, Gianfranco Fioraso, Cinzia Banzato & Jo De Waele (2010) Evolution of karst in Messinian gypsum (Monferrato, Northern Italy), Geodinamica Acta, 23:1-3,29-40, DOI: 10.3166/ga.23.29-40) [61].

1) Geological Characterisation

In the Moncalvo area, where gypsum layers remain undisturbed and stretch over several kilometers, two significant quarries with a combined length of around 1 km have been identified (as shown in Figure 1). These quarries, which form part of the deep groundwater flow system, extend down to 60 meters below the current thalweg levels and were entirely submerged, with the water pressure reaching up to 3 bars. The mining tunnels that were dug into the gypsum intersected these water-filled caves, leading to a forceful surge of water into the mining passages. Following the removal of water from the mine, this quarry network has been explored until reaching a barrier of silty-clay sediments, which nearly fills the entire space.

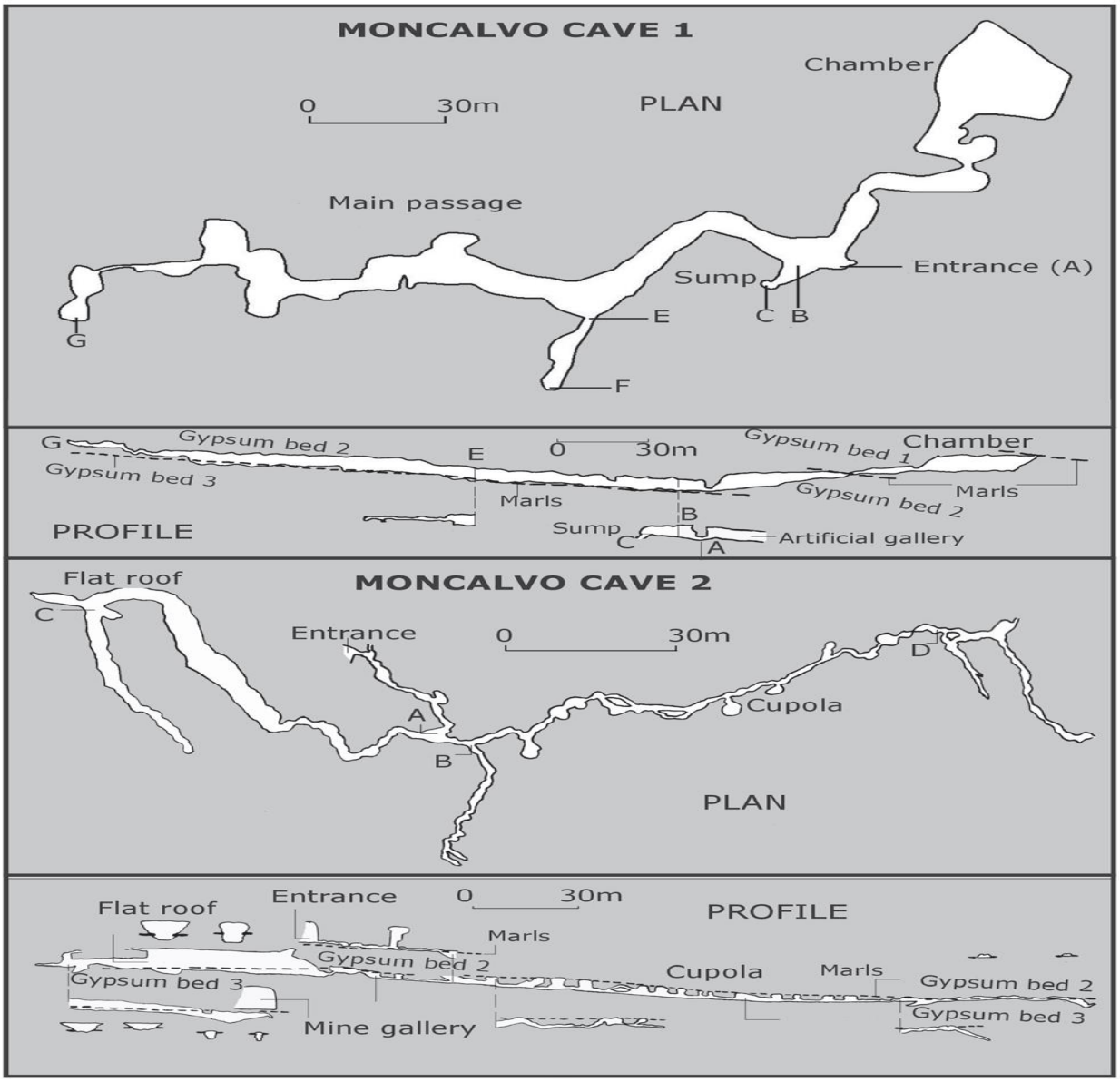

Figure 51 illustrates the overhead view and the longitudinal sections of the two principal quarries in Moncalvo. In these profiles, the layers of marl are depicted with dashed lines. The orientation of the maps places north at the top. These surveys were conducted by the Gruppo Speleologico Piemontese CAI/UGET.(To cite this article: Bartolomeo Vigna, Gianfranco Fioraso, Cinzia Banzato & Jo De Waele (2010) Evolution of karst in Messinian gypsum (Monferrato, Northern Italy), Geodinamica Acta, 23:1-3,29-40, DOI: 10.3166/ga.23.29-40) [62].

2) Sedimentological Characterisation

In the area under investigation, quarry sediments can be categorized into four distinct types: collapse breccias, either massive or laminated clays and silts, massive or layered sands, and extrusion breccias. Of these, collapse breccias are the most frequently encountered sediment type within the surface layer. These breccias consist of a disorganized assortment of polygenic, angular fragments ranging from 0.2 to 2-3 cm, set within a sparse matrix of silty-clay or silty-sand. The fragments are primarily made up of clayey marls

or clays, with occasional small to medium-sized limestone and speleothem pieces. In some cases, gypsum fragments reaching up to 20 cm in length are also present. It is common to find layers or lenses of parallel-stratified silty sands, varying in thickness from centimeters to decimeters, within these breccias [63].

Results obtained of all specimens in the Polito Laboratary.

Specimen	Mass (g)	l.b.h mm3	Volume cm3	Mass volume kg/m3	UCS MPA	Static modulus Mpa	Pundit time us@250kHz/54kHz	Pundit velocity m/s	Dynamic modulus Mpa
FG1	5571	2546412	2.546412	2187	25.75	1840	50	3820	3.19 e10
FG2	4861	2183014	2.183014	2226	30.70	2420	50	4040	3.63 e10
FG3	6652	2995704	2.995704	2220	23.50	1880	46	4500	4.49 e10
CG1	5884	2683560	2.68356	2193	24.40	1740	65-50	2923/3800	1.87 e10/3.16 e10
CG2	6982	3025440	3.02544	2308	21.63	1560	52	3654/4050	3.08 e10/3.78 e10
CG3	5129	2276976	2.276976	2252	26.66	1840	36	4944	5.50 e10

The solubility of gypsum in water, at 0.015 mol/kg H_2O, surpasses that of numerous other minerals. The influence of water on both the mechanical strength and the physical characteristics of gypsum rock is of particular importance in the context of underground excavation activities (Ramon et al., 2021). Gypsum mines are frequently situated beneath the groundwater table's static level, necessitating ongoing water removal to facilitate the creation of underground passages. When mining activities cease, leading to the discontinuation of water pumping efforts, the groundwater levels revert to their original state, causing the gypsum formations to become re-saturated. This process of re-saturation sees water permeating the rock's interconnected porosity, significantly affecting the immediate and prolonged stability of these subterranean mines.

For these reasons, the current study aims to analyze the geomechanical mechanism and karst of gypsum formations in Quarry. We have studied the behavior of gypsum specimens before and after testing, how they differ from each other, their physical strength and rheology of gypsum rock. We also obtained the Uniaxial compressive strength for each specimen, pundit velocity [69].

The results obtained are astonishing as we see the strength of the specimens is quite higher than expected after testing.

CHAPTER 05

5.1 CONCLUSION

A crucial raw material for many other industrial industries as well as building construction is gypsum. The Messinian "Formazione Gessoso Solfifera" (recently renamed "Complesso Caotico di Valle Versa"; Dela Pierre et al., 2003) is the primary group of exploited gypsum formations in Piedmont. It mostly outcrops in the Langhe and Monferrato domains (Tertiary Piedmont Basin). There used to be a lot of open pit and underground gypsum quarries in those locations, but the most have now been closed; the only ones that are still in operation are in Monferrato.

Gypsum extraction has often been linked to environmental and safety issues related to the quarry face, drift stability, and surface subsidence hazard because of its geostructural setting and hydrological properties. Active karst circuits, filling karst voids with water, stratigraphical or structural marly layers, and terrigenous deposits are the major important factors to consider while organizing and managing a quarrying operation.

Geological, structural, and hydrogeological investigations are among the methodological techniques used to ensure appropriate risk management and land planning. These studies are bolstered by hydrological monitoring and geophysical surveys.

The first factor affecting survey program reliability is the deposit's geological asset: the number, distribution, and correlation of mechanical and geophysical surveys are all influenced by the presence of chaotic melange, or irregular gypsum blocks mixed in a matrix of weakly consolidated "mud breccias," or regular gypsum lenses. Furthermore, to confirm face and drift stability and reconstruct the distribution of tensional stresses in the ore body, the geotechnical and geomechanical behavior of the gypsum deposit and marly levels must be precisely defined through appropriate laboratory testing and in situ monitoring activities.

In order to avoid negative effects on the environment and ensure that the gypsum resource is properly exploited under safe circumstances, attention must also be paid to the conservation of water resources and the assessment of hazards associated with the existence of karst activity.
The procedures for a local geostructural survey, geomechanical characterization, and stope monitoring primarily for deformation should always be anticipated in order to provide a safe design.

REFERENCES

1. [1] Bull Eng Geol Environ (2005) 64: 55–65 DOI 10.1007/s10064-004-0270-5 the geological strength index: applications and limitations.
2. [2] Geo-surveying for safe underground mining in gypsum deposit in Monferrato basin (Italy) / BONETTO S; FORNARO M; OGGERI C.. - (2006), pp. 382-387. ((Intervento presentato al convegno MPES2006 tenutosi a Turin nel 20-22 Sept. 2006.
3. [3] Subsidence hazards connected to quarrying activities in a karst area: the case of the Moncalvo sinkhole event (Piedmont, NW Italy) Sabrina Bonettoa, Adriano Fioruccib, Mauro Fornaroa, and Bartolomeo Vignab a University of Torino, 35 via Valperga Caluso, 10125 Torino, Italy; sabrina.bonetto@unito.it, mauro.fornaro@unito.it b Politecnico di Torino, 24 C. so Duca degli Abruzzi, 10129 Torino, Italy; adriano.fiorucci@polito.it, bartolomeo.vigna@polito.it Received 28 December 2007
4. [4] THE GEOLOGICAL STRENGTH INDEX (GSI): A CHARACTERIZATION TOOL FOR ASSESSING ENGINEERING PROPERTIES FOR ROCK MASSES By Paul G. Marinos, Ph.D.,1 Vassilis Marinos,2 and Evert Hoek, Ph.D.3
5. [5] TH E CAVES IN TH E UN DERGROUN D QUARRIES OF MON CALVO D'ASTI – PIEDMONT (ITALY) LE GROTTE NELLE CAVE SOTTERRANEE DI MONCALVO D'ASTI – PIEMONTE (ITALIA) Bartolomeo Vigna1, Jo De Waele2 & Cinzia Banzato1
6. [6] Excavation of a layered rock mass with the use of transverse cutting heads of a roadheader in the light of computer studies Article in Archives of Mining Sciences · January 2018.
7. [7] Stato dell'arte sul rischio Sinkhole nell'area del Basso Monferrato (TO) State of art about Sinkhole in lower Monferrato (TO)
8. [8] GPR surveys for the prevention of karst risk in underground gypsum quarries Chiara Casellea,∗, Sabrina Bonettoa, Cesare Cominaa, Stefano Stoccob a Department of Earth Sciences – DST, Università degli Studi di Torino, via Valperga Caluso 35, Torino 10125, Italy b GAMUT S.r.l., via Lamarmora 16, Torino 10128, Italy.
9. [9] The northernmost record of the Messinian salinity crisis (Piedmont basin, Italy) Article *in* Geological Field Trips · November 2016 DOI: 10.3301/GFT.2016.03
10. [10] Moncucco Torinese, a new post-evaporitic Messinian fossiliferous site from Piedmont (NW Italy) Article in Neues Jahrbuch für Geologie und Paläontologie - Abhandlungen · January 2011 DOI: 10.1127/0077-7749/2010/0108
11. [11] The science of caves and karst: From the beginning of the Geological Society of America to ca. 1960 Chapter · January 2015 DOI: 10.1130/2015.2516(02)
12. [12] Evaluation of Geomechanical Properties of Soft Rock Masses by Laboratory and In Situ Testing Chapter · January 2020 DOI: 10.1007/978-3-030-29477-9_8
13. [13] Messinian karst in Monferrato gypsum areas (North Italy) Conference Paper · January 2009
14. [14] Hypogene gypsum karst and sinkhole formation at Moncalvo (Asti, Italy) Article in Zeitschrift für Geomorphologie Supplementary Issues · May 2010 DOI: 10.1127/0372-8854/2010/0054S2-0015
15. [15] Hypogene Gypsum Caves in Piedmont (N-Italy) Chapter · August 2017 DOI: 10.1007/978-3-319-53348-3_13

16. [16] Effect of Microstructure and Relative Humidity on Strength and Creep of Gypsum Anna Ramon1,2 · Chiara Caselle3 · Sabrina Maria Rita Bonetto3 · Daniele Costanzo4 · Eduardo E. Alonso2 Received: 28 May 2020 / Accepted: 11 May 2021 / Published online: 24 May 2021 © The Author(s) 2021
17. [17] Available online at scholarcommons.usf.edu/ijs International Journal of Speleology Official Journal of Union Internationale de Spéléologie
18. [18] Geo-surveying for safe underground mining in gypsum deposit in Monferrato basin (Italy) S. Bonetto & M . Fornaro Dip. Scienze della Terra, Università degli Studi di Torino, Italy C. Oggeri Dip. Ing. dell'Ambiente, Territorio e Geotecnologie, Politecnico di Torino, Italy
19. [19] Bonsignore G., Bortolami G.C.., Elter G., Montrasio A., Petrucci F., Ragni U., Sacchi R., Sturani C. & Zanella E. (1969). Note Illustartive della Carta geologica d'Italia alla scala 1:100.000; Fogli 56 e 57 Torino-Vercelli. Ercolano: Poligrafica & Cartevalori (Ed.)
20. [20] Dela Pierre F., Piana F., Fioraso G., Boano P., Bicchi E., Forno M.G., Violanti D., Balestro G., Clari P., D'Atri A., D Luca D., Morelli M. & Ruffini R. (2003). Note Illustartive della Carta geologica d'Italia alla scala 1:50.000; Foglio 157 Trino. Settore Studi e ricerche Geologiche – Sistema Informativo Prevenzione Rischi (ARPA). Nichelino: Litografia Geda.
21. [21] Ferrero A.M., Del Greco O., Giani G.P., Ranieri G. & Stragiotti L. (1990). Application of seismic tomography to the rock mass modelling. Mechanics of Jointed and Faulted Rock. Rotterdam: Rossmanith Ed. pp. 129-136.
22. [22] Fioraso G. & Boano P. (2002). Cavità di dissoluzione e fenomeni di sprofondamento nei gessi del Monferrato settentrionale: meccanismi genetici ed effetti sulla stabilità dei versanti. GEAM, 4 (2002): pp. 57-64. Fornaro, M., Lovera, E. & Sacerdote, I. (2002). La coltivazione delle cave ed il recupero ambientale (2 Volumi). Torino: Ed. Politeko.
23. [23] Kirali L. (1969). Anisotropie et hètèrogènèité de la permeabilitè dans le calcaires fissurès. Ecl. Geol. Helv. Louis C. (1969). A study of groundwater fow in jointed rock and its influence on the stability of rock masses. Imperial College Rock Mechanics Research Report. Snow D.T. (1969). Permeability of Crystalline
24. [24] Amalberto, S., Banzato, C., Civita, M., Fiorucci, A. & Vigna, B. 2006. L'inrush nella cava di gesso di Moncalvo (AT). In Proceedings of the GEAM Conference "Le cave in sotterraneo" – 20–21 giugno 2006, Torino, pp. 107 112.
25. [25] Bonetto, S. 2006. Il gesso: da risorsa economica a patrimonio culturale del Monferrato. Aggiornamento tecnico, metodologie operative e ipotesi di riuso dei siti di cava dimessi. Doctorate Thesis, Politecnico di Torino, 447 pp.
26. [26] Bonetto, S. & Fornaro, M. 2005. Subsidence events related to natural conditions and gypsum quarrying activity in the Monferrato area (Piedmont, NW Italy). In Proceedings of MAEGS14 – 14th Meeting of the Association of European Geological Societies, Torino, 19–23 September 2005, pp. 61-62.
27. [27] Bonetto, S., Dino, G. A. & Fornaro, M. 2005. Guide lines for the quarrying exploitation of messinian gypsum deposit: the case of the Monferrato area (Piedmont, NW Italy). In Proceedings of the First International Conference on the Geology of Tethys, 12–14 November, 2005, Cairo University, pp. 209-217.
28. [28] Bonetto, S., Dino, G. A. & Fornaro, M. 2005. Guide lines for the quarrying exploitation of messinian gypsum deposit: the case of the Monferrato area (Piedmont, NW Italy). In Proceedings

of the First International Conference on the Geology of Tethys, 12–14 November, 2005, Cairo University, pp. 209-217.
29. [29] Dela Pierre, F., Piana, F., Fioraso, G., Boano, P., Bicchi, E., Forno, M. G., Violanti, D., Balestro, G., Clari, P., D'atri, A., De Luca, D., Morelli, M. & Ruffini, R. 2003. Note Illustrative della Carta geologica d'Italia alla scala 1 : 50.000; Foglio 157 Trino. Settore Studi e ricerche Geologiche – Sistema Informativo Prevenzione Rischi – ARPA, Litografia Geda, Nichelino, 2003, 147 pp.
30. [30] Fornaro, M., Savasta, G., Accattino, G. & Amalberto, S. 1996. Progetto di una moderna coltivazione di gesso in sotterraneo ed inserimento ambientale dell'attività estrattiva. In IV Congresso Minerario Italo-brasiliano, Canela (Brasile); EGATEA (no. especial), 104-114.
31. [31] Fornaro, M., Innaurato, N., Mancini, R., Amalberto, S. & Pontarollo, J. N. 2000. Kammerauffahrung mit einer Teilschnittmaschine in einer Gipsgrube. In Proceedings of XXIV Symposium of the International Society for Rock Mechanics, Eurock 2000, pp. 501–506. Verlag Glückauf, Essen.
32. [32] Barton N, Lien R, Lunde J [1974]. Engineering classification of rock masses for the design of tunnel support. Rock Mech 6(4):189–236.
33. [33] Cai M, Kaiser PK, Uno H, Tasaka Y, Minami M [2004]. Estimation of rock mass strength and deformation modulus of jointed hard rock masses using the GSI system. Int J Rock Mech Min Sci 41(1):3–19.
34. [34] Chandler RJ, de Freitas MH, Marinos P [2004]. Geotechnical characterization of soils and rocks: a geological perspective. In: Proceedings of the Advances in Geotechnical Engineering: The Skempton Conference. Vol 1.London: Thomas Telford, pp. 67–102.
35. [35] Diederichs MS, Kaiser PK, Eberhardt E [2004]. Damage initiation and propagation in hard rock during tunneling and the influence of near-face stress rotation. Int J Rock Mech Min Sci 41(5):785–812.
36. [36] Essex RJ. [1997]. Geotechnical baseline reports for underground construction. Reston, VA: American Society of Civil Engineers.
37. [37] Hoek E [1994]. Strength of rock and rock masses. News J ISRM 2(2):4–16.
38. [38] Hoek E, Brown ET [1980]. Underground excavations in rock. London: Institution of Mining and Metallurgy.
39. [39] Hoek E, Karzulovic A [2000]. Rock mass properties for surface mines. In: Hustrulid WA, McCarter MK, van Zyl DJA, eds. Slope stability in surface mining. Littleton, CO: Society for Mining, Metallurgy, and Exploration, Inc., pp. 59–70.
40. [40] Hoek E, Caranza-Torres CT, Corkum B [2002]. Hoek- Brown failure criterion. In: Bawden HRW, Curran J, Telsenicki M, eds. Proceedings of the North American Rock Mechanics Society (NARMS–TAC), Mining Innovation and Technology (Toronto, Ontario, Canada), pp. 267–273.
41. [41] Hoek E, Kaiser PK, Bawden WF [1995]. Support of underground excavations in hard rock. Rotterdam, Netherlands: Balkema.
42. [42] Hoek E, Marinos P, Benissi M [1998]. Applicability of the geological strength index (GSI) classification for weak and sheared rock masses: the case of the Athens schist formation. Bull Eng Geol Env 57(2):151–160.
43. [43] Hoek E, Marinos P, Marinos V [2005]. Characterization and engineering properties of tectonically undisturbed but lithologically varied sedimentary rock masses under publication. Int J Rock Mech Min Sci 42:277–285.

44. [44] Knill J [2003]. Core values (first Hans-Closs lecture). Bull Eng Geol Env 62:1–34. Marinos P, Hoek E [2000]. GSI: a geologically friendly tool for rock mass strength estimation. In: Proceedings of GeoEng 2000 at the International Conference on Geotechnical and Geological Engineering (Melbourne, Victoria, Australia). Lancaster, PA: Technomic Publishers, pp. 1422–1446.
45. [45] Marinos P, Hoek E, Marinos V [2006]. Variability of the engineering properties of rock masses quantified by the geological strength index: the case of ophiolites with special emphasis on tunnelling. Bull Eng Geol Env 65:129–142.
46. [46] Palmström A [1996]. Characterizing rock masses by the RMi for use in practical rock engineering. Part 1: the development of the rock mass index (RMi). Tunnelling Undergr Space Technol 11(2):175–88.
47. [47] Rocscience, Inc. [2007]. RocLab v1.0: rock mass strength analysis using the generalized Hoek-Brown failure criterion. [http://www.rocscience.com/products/ RocLab.asp]. Date accessed: April 2007.
48. [48] Sonmez H, Ulusay R [1999]. Modifications to the geological strength index (GSI) and their applicability to the stability of slopes. Int J Rock Mech Min Sci 36:743–760.
49. [49] Tzamos S, Sofianos AI [in press]. A correlation of four rock mass classification systems through their fabric indices. Int J Rock Mech Min Sci.
50. [50] FIORASO G., BICCHI E., IRACE A. & BOANO P. (2004) – Manifestazioni carsiche nelle evaporiti messiniane del Monferrato e della Collina di Torino (Italia nord-occidentale): analisi dei meccanismi genetici nel quadro dell'evoluzione pliocenico-quaternaria del Bacino Terziario Piemontese. Il Quaternario, 17, (2/2): 453-476.
51. [51] FIORUCCI A. & VIGNA B. (2013) - Studio idrogeologico relative alla cava di gesso in sotterraneo "Franca" nel Comune di Calliano di proprietà della Fassa S.p.A. Dipartimento di Ingegneria dell'Ambiente, del Territorio e delle Infrastrutture, Politecnico di Torino, pp. 116, Torino.
52. [52] GALLEANI L., VIGNA B., BANZATO C. & LO RUSSO S. (2011) Validation of a Vulnerability Estimator for Spring Protection Areas: The VESPA index. Journal of Hydrology, 396: 233-245.
53. [53] KLIMCHOUK A. (1996) - The typology of gypsum karst according to its geological and geomorphological evolution. In: Klimchouk A., Lowe D., Cooper A., Sauro U. (Eds.), Gypsum karst of the world. International Journal of Speleology, 25 (3-4): 61-82.
54. [54] MARCHIONATTI F. (2014) – L'integrazione dei grandi scavi in sotterraneo con gli acquiferi. Politecnico di Torino, Tesi di Dottorato di Ricerca in Ambiente e Territorio, pp. 294,Torino.
55. [55] PALMER M.V. & PALMER A.N. (1989) - Paleokarst of the United States. In: P. BOSAK, D.C. FORD, J. GLAZEK & I. HORACEK (Eds.), Paleokarst, a systematic and regional review. Developments in Earth Surface Processes, 1, pp. 725.
56. [56] SACCO F. (1889-1890) - Il Bacino Terziario e Quaternario del Piemonte. In: Atti Società Italiana Scienze Naturali, pp. 624,Torino.
57. [57] VIGNA B. (2007) - Schematizzazione e funzionamento degli acquiferi in rocce carbonatiche. In: Memorie dell'Istituto Italiano di Speleologia - Serie Geologica e Geofisica, 19: 21-26, Bologna.

58. [58] VIGNA B., FIORUCCI A., BANZATO C., FORTI P. & DEWAELE, J. (2010) - Hypogene gypsum karst and sinkhole formation at Moncalvo (Asti, Italy). In: Zeitschrift fur Geomorphologie, 54, (Suppl. 2): 285-306, Stuttgart.
59. [59] Afshar, A., Abedi, M., Norouzi, G.-H., Riahi, M.-A., 2015. Geophysical investigation of underground water content zones using electrical resistivity tomography and ground penetrating radar: a case study in Hesarak-Karaj, Iran. Eng. Geol. 196, 183–193. https://doi.org/10.1016/j.enggeo.2015.07.022.
60. [60] Bonetto, S., Fornaro, M., 2005. Subsidence events related to natural conditions and gypsum quarrying activity in the Monferrato area (Piedmont, NW Italy). Presented at the In Proceedings of MAEGS14 – 14th Meeting of the Association of European Geological Societies, Torino, 19–23 September 2005, pp. 61–62.
61. [61] Caselle, C., Penone, A., Bonetto, S., 2018. Preliminary mechanical characterisation of gypsum rock using UCS and Point Load Test correlation. Geoingegneria Ambientale e Mineraria 153, 60–67.
62. [62] Aloisi G., Pierre C., Rouchy J.M., Foucher J.P., Woodside J. & Party M.S. (2000) - Methane-related authigenic carbonates of eastern Mediterranean Sea mud volcanoes and their possible relation to gas hydrate destabilisation. Earth and Planetary Science Letters, 184, 321-338.
63. [63] Baker P.A. & Kastner M. (1981) - Constraints on the formation of sedimentary dolomite. Science, 213, 214-216. Bailey J.V., Orphan V.J., Joye S.B. & Corsetti F. (2009) - Chemotrophic microbial mats and their potential for preservation in the rock record. Astrobiology, 9, 1-17.
64. [64] Rouchy, J.M.; Caruso, A. The Messinian Salinity Crisis in the Mediterranean Basin: A Reassessment of the Data and an Integrated Scenario. Sediment. Geol. 2006, 188, 35–67. [CrossRef]
65. [65] Manzi, V.; Roveri, M.; Gennari, R.; Bertini, A.; Biffi, U.; Giunta, S.; Iaccarino, S.M.; Lanci, L.; Lugli, S.; Negri, A.; et al.
66. [66] Deep-Water Counterpart of the Messinian Lower Evaporites in the Apennine Foredeep: The Fanantello Section (Northern Apennines, Italy). Palaeogeogr. Palaeoclimatol. Palaeoecol. **2007**, 251, 470–499. [CrossRef]
67. [67] Dela Pierre, F.; Bernardi, E.; Cavagna, S.; Clari, P.; Gennari, R.; Irace, A.; Lozar, F.; Lugli, S.; Manzi, V.; Natalicchio, M.; et al. The Record of the Messinian Salinity Crisis in the Tertiary Piedmont Basin (NW Italy): The Alba Section Revisited. Palaeogeogr. Palaeoclimatol. Palaeoecol. 2011, 310, 238–255. [CrossRef].
68. [68] Journal of Structural ,Geology, Volume 163, October 2022, 104722, Influence of water on deformation and failure of gypsum rock.
69. [69]Engineering Geology, Volume 74, August 2004, pages 183-196, The aging of gypsum in underground mines